Dopamine projections to the basolateral amygdala drive the encoding of identity-specific reward memories

Ana C. Sias[1], Yousif Jafar[1], Caitlin M. Goodpaster[1], Kathia Ramírez-Armenta[1], Tyler M. Wrenn[1], Nicholas K. Griffin[1], Melissa J. Sharpe[1-4], Kate M. Wassum[1-4]

[1]Dept. of Psychology, UCLA, Los Angeles, CA 90095. [2]Brain Research Institute, UCLA, Los Angeles, CA 90095, USA. [3]Integrative Center for Learning and Memory, University of California Los Angeles, Los Angeles, CA, USA. [4]Integrative Center for Addictive Disorders, University of California Los Angeles, Los Angeles, CA, USA.

Correspondence:
Kate Wassum: kwassum@ucla.edu
Dept. of Psychology, UCLA
1285 Franz Hall
Box 951563
Los Angeles, CA 90095-1563

Short title: VTA_{DA}→BLA projections drive stimulus-outcome learning

Key words: learning, memory, decision making, Pavlovian conditioning, Pavlovian-to-instrumental transfer, ventral tegmental area, basolateral amygdala, appetitive, model-based learning

Figures: 5
Tables: 0
Supplemental Tables: 0
Supplemental Figures: 7
Words:
Abstract: 150
Main Text: 3750

ABSTRACT

To make adaptive decisions, we build an internal model of associative relationships in the environment and use it to predict specific forthcoming outcomes. Detailed stimulus-outcome memories are a core feature of such cognitive maps, yet little is known of the neuronal systems that support their encoding. We used fiber photometry, cell-type and pathway-specific optogenetic manipulation, Pavlovian cue-reward conditioning, and a decision-making test in male and female rats, to reveal that ventral tegmental area dopamine (VTA_{DA}) projections to the basolateral amygdala (BLA) drive the encoding of stimulus-outcome memories. Dopamine is released in the BLA during stimulus-outcome pairing and VTA_{DA}→BLA activity is necessary and sufficient to link the identifying features of a reward to a predictive cue, but does not mediate general value or reinforcement. These data reveal a dopaminergic pathway for the learning that supports adaptive decision making and help understand how VTA_{DA} neurons achieve their emerging multifaceted role in learning.

Dopamine has long been known to critically contribute to learning. The canonical view is that midbrain dopamine neurons broadcast errors in reward prediction. These learning signals are thought to cache the general value of a reward to its predictor and reinforce response policies that rely on past success, rather than forethought of specific outcomes[1-7]. But often adaptive decision making requires accurate and detailed prospective consideration of potential outcomes. For example, if you see both pizza and donut boxes outside the seminar room, assuming you like both, you need to use these cues to represent the specific predicted foods in order to make the snack choice that is optimal in your current circumstances (e.g., are you craving something sweet or savory?). So, to ensure flexible behavior, humans and other animals do not just learn the general value of predictive events, but also encode the relationships between these cues and the identifying features of their associated outcomes[8, 9]. Such stimulus-outcome memories are fundamental components of the internal model of environmental relationships, aka cognitive map[10], we use to generate the predictions and inferences needed for many forms of flexible, advantageous decision making[8, 9, 11, 12]. Although there is little known of how we form stimulus-outcome memories, recent evidence suggests dopamine might actually contribute[13-24]. New data have challenged the value-centric dogma of dopamine function, indicating it plays a much broader role in learning than originally thought[25-29]. How dopamine contributes to identity-specific stimulus-outcome learning is unknown, yet critical for understanding dopamine's emerging multifaceted function in learning.

One candidate pathway through which dopamine might contribute to stimulus-outcome learning is the VTA dopamine (VTA_{DA}) projection to the basolateral amygdala (BLA)[30-35]. This pathway has received much less attention than the canonical VTA_{DA} projections to nucleus accumbens and prefrontal cortex, so little is known of its function. VTA_{DA}→BLA projections do contribute to Pavlovian fear learning[32], yet whether this pathway also contributes to appetitive learning and the type and content of the memories supported are unknown. The BLA itself was recently shown to be crucial for forming detailed, identity-specific, appetitive, stimulus-outcome memories[36]. Therefore, here we combined a systems neuroscience toolkit with sophisticated behavioral tasks to evaluate VTA_{DA}→BLA pathway function in linking the unique features of rewarding events to predictive cues, i.e., encoding the identity-specific reward memories that support flexible decision making.

RESULTS

BLA neurons are active during stimulus-outcome learning.

We first asked whether and when the BLA is active during the encoding of detailed, identity-specific stimulus-outcome memories. To characterize the endogenous activity of BLA neurons, we used fiber photometry to record fluorescent activity of the genetically encoded calcium indicator GCaMP6f[37] in the BLA of male and female rats (Figure 1a-b). Rats were food deprived and received 8 sessions of Pavlovian conditioning during which 2 distinct auditory conditioned stimuli (CS) each predicted a unique food reward

(e.g., white noise—sucrose/click—pellets). During each session, each cue was presented 8 times (variable 2.5-min mean intertrial interval, ITI) for 30 s and terminated in the delivery of its associated reward (Figure 1c). This conditioning has been shown to engender the encoding of identity-specific stimulus-outcome memories as evidenced by the ability of the cues to subsequently promote instrumental choice of their specific predicted reward[38-42] and sensitivity of the conditional goal-approach response to devaluation of the predicted reward[43]. Across training, rats developed a Pavlovian conditional approach response of entering the food-delivery port during cue presentation (Figure 1d).

BLA neurons are active during the encoding of stimulus-outcome memories. Fiber photometry recordings were made during Pavlovian conditioning and binned into five conditioning phases: Session 1, 2, 3/4, 5/6, and 7/8. Thus, data from the last 6 sessions were averaged across 2-session bins. BLA neurons were robustly activated both at cue onset and offset when the outcome was delivered. BLA responses to cue offset/reward delivery were larger than those to cue onset and increased with training (Figure 1e-f; see also Supplemental Figure 1-1 for data from each of the 8 training sessions). Thus, consistent with prior evidence[36], BLA neurons are activated by rewards and their predictors. BLA activation is particularly robust during the critical outcome period when the cues can become linked to the identifying features of the outcomes they predict.

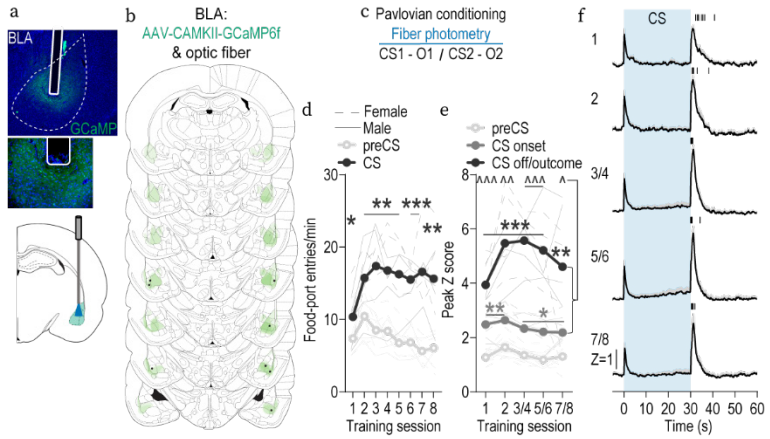

Figure 1. BLA neurons are active during stimulus-outcome encoding. (a) Top: Representative fluorescent image of GCaMP6f expression and fiber placement in the BLA. Bottom: Schematic of fiber photometry approach for imaging bulk calcium activity in BLA neurons. **(b)** Schematic representation of GCaMP6f expression and placement of optical fiber tips in BLA for all subjects. Brain slides from[44]. **(c)** Procedure schematic. CS, conditioned stimulus (white noise or click); O, outcome (sucrose solution or grain pellet). **(d)** Food-port entry rate during the CS relative to the preCS baseline period, averaged across trials and across the 2 CSs for each day of Pavlovian conditioning. Thin lines represent individual subjects. Training x CS: $F_{(2.44, 17.07)}$ = 7.97, P = 0.002; Training: $F_{(3.30, 23.10)}$ = 4.85, P = 0.008; CS: $F_{(1, 7)}$ = 80.33, P < 0.0001. *P < 0.05, **P < 0.01, ***P < 0.001 relative to preCS, Bonferroni correction. **(e)** Trial-averaged quantification of maximal (peak) GCaMP6f Z-score ΔF/F during the 5-s period following CS onset or outcome delivery compared to the equivalent baseline period immediately prior to CS onset. Training x Event: $F_{(2.52, 17.61)}$ = 3.94, P = 0.03; Event: $F_{(1.39, 9.71)}$ = 58.63, P < 0.0001; Training $F_{(1.71, 11.97)}$ = 2.30, P = 0.15. *P < 0.05, **P < 0.01, ***P < 0.001 relative to preCS baseline, Bonferroni correction. ^ P < 0.05, ^^ P < 0.01, ^^^ P < 0.001 CS offset/outcome relative to CS onset, Bonferroni correction. **(f)** Trial-averaged GCaMP6f fluorescence changes (Z-score ΔF/F) in response to CS presentation (blue box) and outcome delivery across days of training. Shading reflects between-subjects s.e.m. Tick marks represent time of outcome collection for each subject. Data from the last six sessions were averaged across two-session bins (3/4, 5/6, and 7/8). N = 8, 4 male.

Dopamine is released in the BLA during stimulus-outcome learning.

We next asked whether dopamine is released in the BLA during the encoding of identity-specific stimulus-outcome memories. We used fiber photometry to record fluorescent activity of the G-protein-coupled receptor-activation-based dopamine sensor $GRAB_{DA2h}$[45] in the BLA of male and female rats during Pavlovian conditioning, as described above (Figure 2a-c). Across training, rats developed a Pavlovian conditional goal-approach response (Figure 2d). BLA neurons were activated both at cue onset and offset/outcome delivery across training (Figure 2e-f; see also Supplemental Figure 2-1 for data from each of the 8 training sessions and Supplemental Figure 2-2 for GFP control). Like BLA neuronal responses, BLA dopamine responses to cue offset/outcome delivery were larger than those to cue onset. After learning, dopamine responses to cue offset were smaller when the outcome was omitted relative to when the outcome was delivered (Supplemental Figure 2-3), indicating reward outcome experience triggers dopamine release in the BLA. Indeed, BLA dopamine was also evoked by unexpected reward delivery (Supplemental Figure 2-3). Thus, dopamine is released in the BLA in response to both cues and rewarding outcomes, as well as their pairing during Pavlovian conditioning. BLA dopamine release is particularly robust at cue offset/outcome delivery, the critical window for encoding stimulus-outcome associations and when BLA neurons are also active.

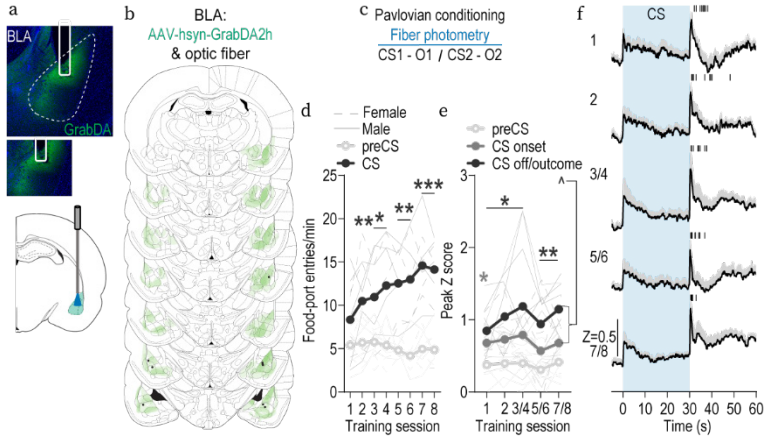

Figure 2. Dopamine is released in the BLA during stimulus-outcome encoding. (a) Top: Representative fluorescent image of GrabDA2h expression and fiber placement in the BLA. Bottom: Schematic of fiber photometry approach for imaging GrabDA2h fluorescence changes in BLA neurons. **(b)** Schematic representation of GrabDA2h expression and placement of optical fiber tips in BLA for all subjects. **(c)** Procedure schematic. CS, conditioned stimulus (white noise or click); O, outcome (sucrose solution or grain pellet). **(d)** Food-port entry rate during the CS relative to the preCS baseline period, averaged across trials and across the 2 CSs for each day of Pavlovian conditioning. Thin lines represent individual subjects. Training x CS: $F_{(2.77, 22.15)}$ = 14.69, P < 0.0001; Training: $F_{(4.75, 38.02)}$ = 2.76, P = 0.03; CS: $F_{(1, 8)}$ = 44.00, P = 0.0002. *P < 0.05, **P < 0.01, ***P < 0.001 relative to preCS, Bonferroni correction. **(e)** Trial-averaged quantification of maximal (peak) GrabDA2h fluorescence change Z-score during the 5-s period following CS onset or outcome delivery compared to the equivalent baseline period immediately prior to CS onset. Event: $F_{(1.89, 15.08)}$ = 16.07, P = 0.0002; Training: $F_{(2.14, 17.14)}$ = 1.07, P = 0.37; Training x Event: $F_{(3.79, 30.35)}$ = 0.84, P = 0.51. * P < 0.05, ** P < 0.01, relative to preCS baseline, Bonferroni correction. ^ P < 0.05 CS offset/outcome relative to CS onset, Bonferroni correction. **(f)** Trial-averaged GrabDA fluorescence changes (Z-score) in response to CS presentation (blue box) and outcome delivery across days of training. Shading reflects between-subjects s.e.m. Tick marks represent time of outcome collection for each subject. Data from the last six sessions were averaged across two-session bins (3/4, 5/6, and 7/8). N = 9, 5 male.

VTA_{DA}→BLA projections are necessary for encoding identity-specific stimulus-outcome memories.

Having found that dopamine is released in the BLA during stimulus-outcome pairing, we next asked whether dopaminergic input to the BLA mediates the encoding of identity-specific stimulus-outcome memories (Figure 3a-d). We expressed the inhibitory opsin archaerhodopsin T (ArchT) or tdTomato control bilaterally in VTA_{DA} neurons of male and female tyrosine hydroxylase (Th)-cre rats[46] (Figure 3a-b) and implanted optical fibers bilaterally over BLA (Figure 3c) to allow us to, in ArchT-expressing subjects, transiently inactivate VTA_{DA} axons and terminals in the BLA. Rats first received 11 days of instrumental conditioning, without manipulation, in which one of two different lever-press actions each earned one of two distinct food rewards (e.g., left press→sucrose/right press→pellets; Figure 3e). Rats then received Pavlovian conditioning. During each of the 8 Pavlovian conditioning sessions, each of 2 distinct, 30-s, auditory cues was presented 8 times and terminated in the delivery of one of the food rewards into a single food port (e.g., white noise—sucrose/click—pellets). VTA_{DA}→BLA projections were optically inhibited (532 nm, 10 mW, 3 s continuous) coincident with each outcome delivery during each Pavlovian conditioning session. We restricted optical inhibition to outcome delivery because this is the time at which the stimulus-outcome pairing occurs and when we detected robust BLA neuron activation and dopamine release in the BLA. Optical inhibition of VTA_{DA}→BLA projections did not disrupt outcome collection (Supplemental Figure 3-1). It also did not impede the development of a Pavlovian conditional goal-approach response (Figure 3f). Thus, VTA_{DA}→BLA projections are not required to reinforce an appetitive Pavlovian response.

Conditional approach to the shared goal location does not require subjects to have learned the identifying details of the predicted rewards. So, to ask whether VTA_{DA}→BLA are needed for encoding identity-specific stimulus-outcome memories, we next gave subjects an outcome-specific Pavlovian-to-instrumental transfer (PIT) test. During this test both levers were present, but lever pressing was not reinforced. Each cue was presented 4 times (also without accompanying outcome), with intervening cue-free baseline periods (fixed 2.5-min ITI), to assess its influence on action performance and selection in the novel choice scenario. Because the cues are never directly associated with the instrumental actions, this test assesses the ability to use the cues to retrieve a representation of the specific predicted outcome to motivate choice of the action known to earn that same unique reward[39, 47, 48]. No manipulation was given on test. If subjects had encoded identity-specific stimulus-outcome memories, then cue presentation should cause them to increase presses selectively on the lever that, during training, earned the same specific outcome as predicted by that cue. Controls showed this outcome-specific PIT effect. Conversely, the cues were not capable of guiding lever-press choice in the group for which VTA_{DA}→BLA projections were inhibited during Pavlovian conditioning (Figure 3g-h). Rather, for these subjects, the cues caused a general increase in lever pressing. As in training, during the PIT test the conditional goal-

approach response was similar between groups (Figure 3i). Thus, VTA_{DA}→BLA projections are active at the time of stimulus-outcome pairing and this activity is needed to link the identifying details of the outcome to the predictive cue, but not to reinforce a conditional response or to assign general value to the cue to support general motivation.

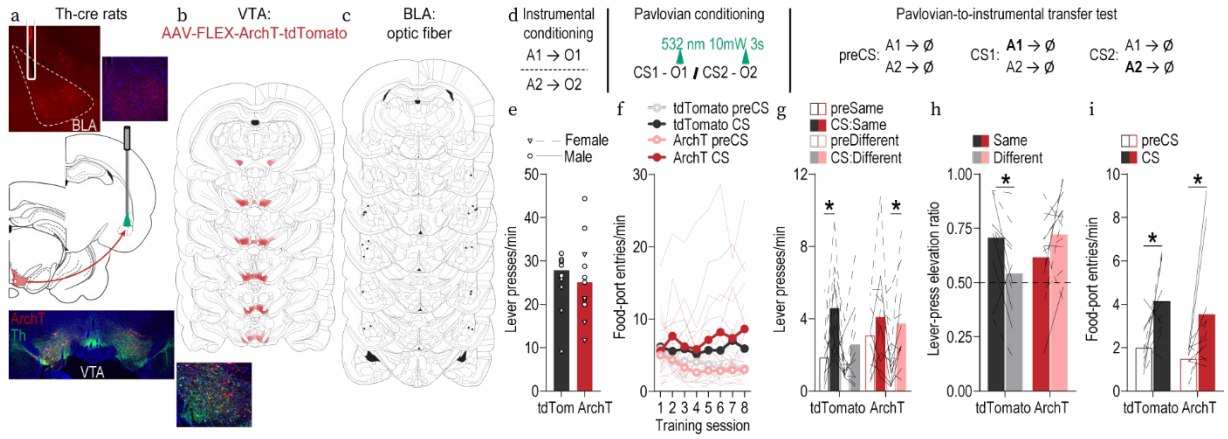

Figure 3. Optical inhibition of VTA_{DA}→BLA projections during stimulus-outcome pairing attenuates the encoding of identity-specific stimulus-outcome memories. (a) Bottom: Representative fluorescent image of cre-dependent ArchT-tdTomato expression in VTA cell bodies with coexpression in Th of Th-Cre rats. Middle: Schematic of optogenetic strategy for bilateral inhibition of VTA_{DA} axons and terminals in the BLA of Th-cre rats. Top: Representative image of fiber placement in the vicinity of immunofluorescent ArchT-tdTomato-expressing VTA_{DA} axons and terminals in the BLA. **(b)** Schematic representation of cre-dependent ArchT-tdTomato expression in VTA and **(c)** placement of optical fiber tips in BLA for all subjects. **(d)** Procedure schematic. A, action (left or right lever press); O, outcome (sucrose solution or grain pellet); CS, conditioned stimulus (white noise or click). **(e)** Instrumental conditioning. Lever-press rate averaged across levers and across the final 2 days of instrumental conditioning. $t_{(19)} = 0.07$, $P = 0.94$. Data points represent individual subjects. **(f)** Pavlovian conditioning. Food-port entry rate during the CS relative to the preCS baseline period, averaged across trials and across the 2 CSs for each day of Pavlovian conditioning. Thin lines represent individual subjects. Training x CS period: $F_{(4.09, 77.71)} = 5.73$, $P = 0.0004$; CS period: $F_{(1,19)} = 10.34$, $P = 0.005$; Training: $F_{(1.47, 27.98)} = 1.19$, $P = 0.31$; Virus: $F_{(1,19)} = 0.05$, $P = 0.83$; Training x Virus: $F_{(7,133)} = 1.23$, $P = 0.29$; Virus x CS period: $F_{(1,19)} = 1.04$, $P = 0.32$; Training x Virus x CS period: $F_{(7,133)} = 0.75$, $P = 0.63$. **(g-i)** Outcome-specific Pavlovian-to-instrumental transfer test. **(g)** Trial-averaged lever-press rates during the preCS baseline periods compared to press rates during the CS periods separated for presses on the lever that, in training, delivered the same outcome as predicted by the CS (Same) and pressing on the other available lever (Different). Virus: $F_{(1, 19)} = 0.93$, $P = 0.35$; Lever: $F_{(1, 19)} = 3.36$, $P = 0.08$; CS period: $F_{(1, 19)} = 22.02$, $P = 0.0002$; Virus x Lever: $F_{(1, 19)} = 0.12$, $P = 0.73$; Virus x CS period: $F_{(1, 19)} = 0.37$, $P = 0.55$; Lever x CS period: $F_{(1, 19)} = 0.25$, $P = 0.62$; Virus x Lever x CS period: $F_{(1, 19)} = 2.63$, $P = 0.12$. $^*P < 0.05$, planned comparisons CS same presses v. preCS same presses and CS different presses v. preCS different presses. **(h)** Elevation in lever presses on the lever that earned the same outcome as the presented CS (Same; [(Same lever presses during CS)/(Same presses during CS + Same presses during preCS)], averaged across trials and across CSs), relative to the elevation in pressing on the alternate lever (Different; [(Different lever presses during CS)/(Different presses during CS + Different presses during preCS)], averaged across trials and across CSs) during the PIT test. Virus x Lever: $F_{(1, 19)} = 9.22$, $P = 0.007$; Virus: $F_{(1, 19)} = 0.33$, $P = 0.57$; Lever: $F_{(1, 19)} = 0.45$, $P = 0.51$. $^*P < 0.05$, Bonferroni correction. Lines represent individual subjects. **(i)** Food-port entry rate during the CSs relative to the preCS baseline periods, averaged across trials and across the 2 CSs during the PIT test. CS period: $F_{(1, 19)} = 15.18$, $P = 0.001$; Virus: $F_{(1, 19)} = 1.15$, $P = 0.30$; Virus x CS period: $F_{(1, 19)} = 0.008$, $P = 0.93$. $^*P < 0.05$, Bonferroni correction. ArchT, $N = 11$, 6 males; tdTomato, $N = 10$, 5 males.

VTA_{DA}→BLA projection activity is sufficient to drive the encoding of identity-specific stimulus-outcome memories.

If VTA_{DA}→BLA projection activity during stimulus-outcome pairing mediates the encoding identity-specific stimulus-outcome memories, we reasoned that activation of these projections should be sufficient to drive the formation of a stimulus-outcome memory. To test this, we first needed to behaviorally attenuate the encoding of stimulus-outcome memories to serve as a platform to neurobiologically rescue such learning.

To achieve this, we took advantage of classic Kamin blocking procedures[49-51]. We asked whether the presence of a cue that already reliably predicts a particular outcome could effectively block formation of an association between a novel cue and the specific features of that outcome[52]. Male and female rats first received instrumental conditioning in which each of two lever-press actions earned a unique food reward (e.g., left press→sucrose/right press→pellets; Figure 4b). Subjects then received 12 visual cue Pavlovian conditioning sessions. For subjects in the Blocking group, during each Pavlovian conditioning session 2 distinct 30 s visual cues each terminated in the delivery of a unique food outcome (e.g., house light—sucrose/flashing light—pellet; 16 of each CS/session; 2.5-min mean variable ITI). Controls received equated training, but with a visual stimulus different from those used for the blocking group. Subjects acquired Pavlovian conditional goal-approach responses to these visual cues (Figure 4c). All subjects then received compound conditioning, during which each of the 2 visual cues previously conditioned for the Blocking group was presented concurrent with an auditory cue for 30 s terminating in the delivery of one of the distinct food outcomes (e.g., house light + white noise—sucrose/flashing light + clicker—pellet; 8 of each compound cue/session). For subjects in the blocking group, each compound cue was paired with the outcome previously associated with the visual stimulus. Thus, the visual component of the compound cue already reliably predicted the outcome. However, for the controls neither the visual nor auditory component of the compound cue had been previously associated with the outcome. All subjects showed conditional goal-approach responses to the compound cues across the 4 compound sessions (Figure 4d). To assess acquisition of the unique auditory stimulus-outcome relationships, rats were given a PIT test in which action selection was evaluated in the presence of the auditory cues alone. If the previously encoded visual stimulus-outcome memory blocked encoding of the relationship between the novel auditory cue and identifying features of the outcome, then subjects in the blocking group should not be able to use the auditory cues to represent the specific predicted outcome and guide their choices towards the action associated with that reward during the PIT test. This is what we found. Whereas controls were able to express outcome-selective PIT, subjects in the blocking group were impaired in their ability to use the auditory cues to guide choice (Figure 4e-f). Despite disrupted PIT performance, expression of conditional goal-approach response was preserved in the blocking group (Figure 4g). Thus, we were able to effectively attenuate the encoding of identity-specific stimulus-outcome memories. More broadly, these data indicate that previously learned predictive cues can prevent encoding of associations between new cues and the identifying features of the predicted events.

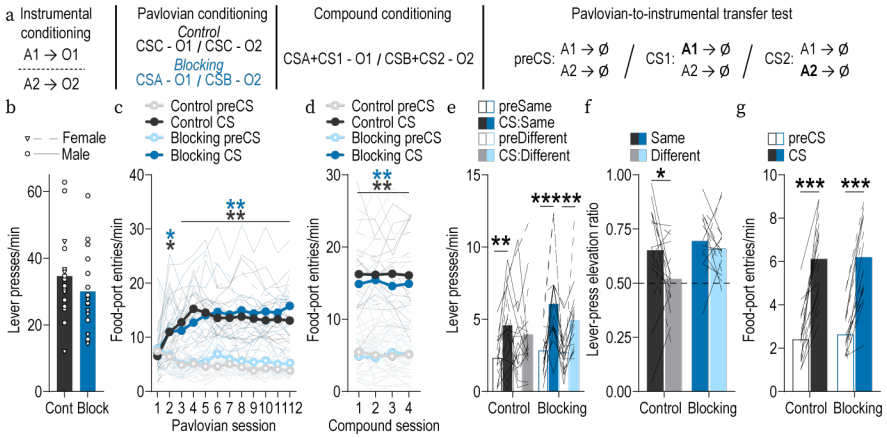

Figure 4. Pre-learned stimulus-outcome relationships block encoding of new identity-specific stimulus-outcome memories. (a) Procedure schematic. A, action (left or right lever press); O, outcome (sucrose solution or grain pellet); CS, conditioned stimulus (CSA/B: house light or flashing lights; CSC: alternating outside lights; CS1/CS2: white noise or click). **(b)** Instrumental conditioning. Lever-press rate averaged across levers and across the final 2 days of instrumental conditioning. $t_{(30)}$ = 1.03, P = 0.31. **(c)** Pavlovian conditioning. Food-port entry rate during the visual CSs relative to the preCS baseline periods, averaged across trials and across CSs for each day of Pavlovian conditioning. Thin lines represent individual subjects. Training: $F_{(2.71, 81.41)}$ = 4.29, P = 0.009; CS period: $F_{(1, 30)}$ = 186.20, P < 0.0001; Group: $F_{(1, 30)}$ = 0.56, P = 0.46; Training x Group: $F_{(11, 330)}$ = 1.77, p=0.06; Training x CS period: $F_{(4.55, 136.40)}$ = 30.77, P < 0.0001; Group x CS period: $F_{(1, 30)}$ = 0.22, p=0.64; Session x Group x CS period: $F_{(11, 330)}$ = 0.98, P = 0.47. * P < 0.05, **P < 0.01, Bonferroni correction. **(d)** Compound conditioning. Food-port entry rate during the compound CSs relative to the preCS baseline periods, averaged across trials and across the 2 compound CSs for each day of compound conditioning. CS period: $F_{(1,30)}$ = 173.60, P < 0.0001; Training: $F_{(1.32, 39.71)}$ = 0.01, P = 0.96; Group: $F_{(1, 30)}$ = 0.35, P = 0.56; Training x Group: $F_{(3, 90)}$ = 0.12, P = 0.95; Training x CS period: $F_{(2.50, 75.01)}$ = 0.50, P = 0.65; Group x CS: $F_{(1, 30)}$ = 0.51, P = 0.48; Training x Group x CS: $F_{(3, 90)}$ = 0.89, P = 0.45. **P < 0.01, Bonferroni correction **(e-g)** Auditory CS outcome-specific Pavlovian-to-instrumental transfer test. **(e)** Trial-averaged lever-press rates during preCS baseline periods compared to press rates during the auditory CS periods separated for presses on the lever that, in training, delivered the same outcome as predicted by the auditory CS (Same) and pressing on the other available lever (Different). Group x CS: $F_{(1, 30)}$ = 4.54, P = 0.04; Lever x CS: $F_{(1,30)}$ = 6.24, P = 0.02; CS period: $F_{(1,30)}$ = 29.11, P < 0.0001; Group: $F_{(1, 30)}$ = 0.59, P = 0.45; Lever: $F_{(1,30)}$ = 0.06, P = 0.81; Group x Lever: $F_{(1, 30)}$ = 2.09, P = 0.16; Group x Lever x CS: $F_{(1, 30)}$ = 0.81, P = 0.38. **P < 0.01, ***P < 0.001 planned comparisons CS same presses v. preCS same presses and CS different presses v. preCS different presses. **(f)** Elevation in lever presses on the lever that earned the same outcome as the presented CS (Same; [(Same lever presses during CS)/(Same presses during CS + Same presses during preCS)], averaged across trials and across CSs), relative to the elevation in presses on the alternate lever (Different; [(Different lever presses during CS)/(Different presses during CS + Different presses during preCS)], averaged across trials and across CSs) during the PIT test. Lines represent individual subjects. Group: $F_{(1, 30)}$ = 3.99, P = 0.06; Lever: $F_{(1, 30)}$ = 4.35, P = 0.046; Group x Lever: $F_{(1, 30)}$ = 1.57, P = 0.22. *P < 0.05, Bonferroni correction. **(g)** Food-port entry rate during the CSs relative to the preCS baseline periods, averaged across trials and across the 2 CSs during the PIT test. CS period: $F_{(1, 30)}$ = 154.70, P < 0.0001; Group: $F_{(1, 30)}$ = 0.10, P = 0.75; Group x CS: $F_{(1, 30)}$ = 0.06, P = 0.80. ***P < 0.001, Bonferroni correction. Blocking, N = 16, 11 males; Control, N = 16, 11 males.

Using this blocking procedure, we next asked whether activation of VTA_{DA}→BLA projections is sufficient to rescue, or unblock, the encoding of identity-specific stimulus-outcome memories (Figure 5a-d). We expressed the excitatory opsin channelrhodopsin (ChR2) or eYFP control in VTA_{DA} neurons of male and female Th-cre rats (Figure 5a-b) and implanted optical fibers bilaterally over BLA (Figure 5c) to allow us to, in ChR2-expressing subjects, transiently stimulate VTA_{DA} axons and terminals in the BLA. Rats first received instrumental conditioning, without manipulation, to learn two action-reward relationships (Figure 5e). They then received visual cue Pavlovian conditioning, also manipulation-free. All subjects received blocking conditions and, thus, during Pavlovian conditioning had two distinct visual cues each paired with a unique food outcome. Both groups developed Pavlovian conditional goal-approach responses to the visual cues (Figure 5f). Rats next received compound conditioning during which each of the visual cues was presented concurrent with an auditory cue for 30 s terminating in the

delivery of the same outcome the visual cue previously predicted. During each compound conditioning session, VTA_{DA}→BLA projections were optically stimulated (473 nm; 20 Hz, 10 mW, 25-ms pulse width, 3 s) at the time of outcome delivery. We selected this stimulation period because it is when the stimulus-outcome pairing and, thus, learning can occur. VTA_{DA}→BLA stimulation had no effect on outcome collection (Supplemental Figure 5-1). It also did not affect goal-approach responses to the compound cue (Figure 5g). To ask about the encoded identity-specific stimulus-outcome memories, we gave rats a PIT test with the auditory cues, without manipulation. We replicated the blocking of identity-specific stimulus-outcome memories in the eYFP controls. These subjects were unable to use the auditory cues to guide their choice behavior during the PIT test. Stimulation of VTA_{DA}→BLA projections during compound training did, however, drive the encoding of identity-specific stimulus-outcome memories. Rats in this group were able to use the auditory cues to know which specific outcome was predicted to bias presses towards the lever associated with that same reward (Figure 5h-i). As in compound conditioning, both groups showed similar goal-approach responses to the cues (Figure 5j), indicating that optical stimulation of VTA_{DA}→BLA projections did not augment reinforcement of a general conditional approach response. Similarly, rats did not self-stimulate VTA_{DA}→BLA projections, indicating stimulation at this frequency, which reflects the upper end endogenous firing rate of dopamine neurons in response to rewarding events [1, 6, 53], was not itself reinforcing (Supplemental Figure 5-2). Thus, activation of VTA_{DA}→BLA projections concurrent with outcome experience is sufficient to drive the encoding of identity-specific stimulus-outcome memories but does not promote reinforcement.

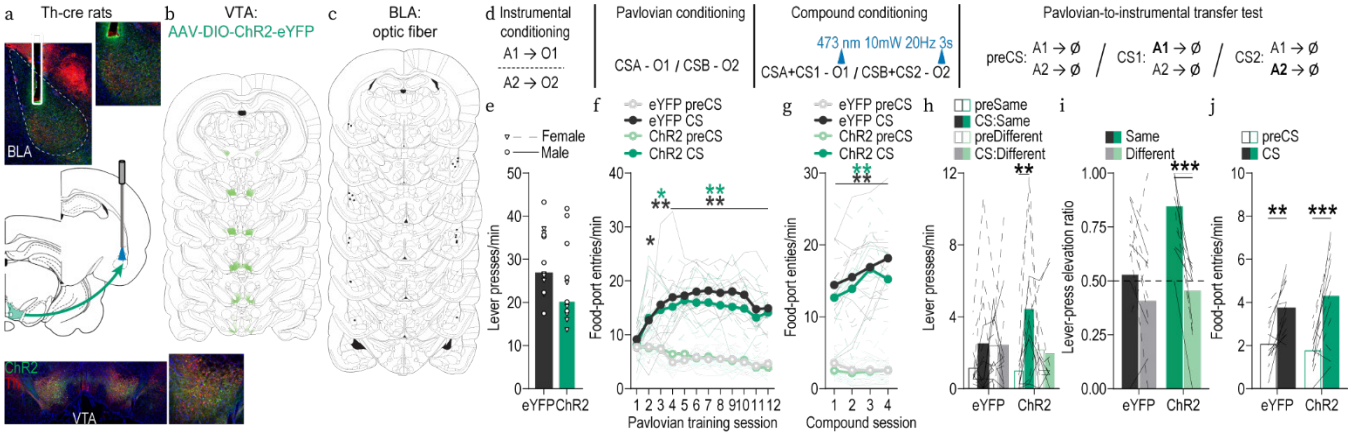

Figure 5. Optical stimulation of VTA_{DA}→BLA projections during stimulus-outcome pairing unblocks encoding of identity-specific stimulus-outcome memories. (a) Bottom: Representative fluorescent image of cre-dependent ChR2-eYFP expression in VTA cell bodies with co-expression of Th in Th-Cre rats. Middle: Schematic of optogenetic strategy for bilateral stimulation of VTA_{DA} axons and terminals in the BLA. Top: Representative image of fiber placement in the vicinity of immunofluorescent ChR2-eYFP-expressing VTA_{DA} axons and terminals in the BLA. **(b)** Schematic representation of cre-dependent ChR2-eYFP expression in VTA and **(c)** placement of optical fiber tips in BLA for all subjects. **(d)** Procedure schematic. A, action (left or right lever press); O, outcome (sucrose solution or grain pellet); CS, conditioned stimulus (CSA/B: house light or flashing lights; CS1/CS2: white noise or click). **(e)** Instrumental conditioning. Lever-press rate averaged across levers and across the final 2 days of instrumental conditioning. $t_{(22)} = 1.39$, $P = 0.18$. **(f)** Pavlovian conditioning. Food-port entry rate during the visual CSs relative to the preCS baseline periods, averaged across trials and across the 2 visual CSs for each day of Pavlovian conditioning. Thin lines represent individual subjects. Training x CS: $F_{(4.15, 91.32)} = 25.86$, $P < 0.0001$; Training: $F_{(2.60, 57.21)} = 7.22$, $P = 0.0006$; CS period: $F_{(1, 22)} = 264.70$, $P < 0.0001$; Virus: $F_{(1, 22)} = 0.67$, $P = 0.42$; Training x Virus: $F_{(11, 242)} = 0.47$, $P = 0.92$; Virus x CS period: $F_{(1, 22)} = 2.24$, p=0.15; Training x Virus x CS period: $F_{(11, 242)} = 0.86$, $P = 0.58$. *$P < 0.05$, **$P < 0.01$,

Bonferroni correction. **(g)** Compound conditioning. Food-port entry rate during the compound CSs relative to the preCS periods, averaged across trials and across the 2 compound CSs for each day of compound conditioning. Training x CS period: $F_{(2.28, 50.21)} = 9.06$, $P = 0.0002$; Training: $F_{(1.35, 29.67)} = 6.43$, $P = 0.01$; CS period: $F_{(1, 22)} = 232.10$, $P < 0.0001$; Virus: $F_{(1, 22)} = 0.88$, $P = 0.36$; Training x Virus: $F_{(3, 66)} = 1.01$, $P = 0.40$; Virus x CS: $F_{(1, 22)} = 0.54$, $P = 0.47$; Training x Virus x CS period: $F_{(3, 66)} = 1.07$, $P = 0.37$ $^{**}P < 0.01$, Bonferroni correction **(h-j)** Auditory CS outcome-specific Pavlovian-to-instrumental transfer test. **(h)** Trial-averaged lever-press rates during the preCS baseline periods compared to press rates during the auditory CSs separated for presses on the lever that, in training, delivered the same outcome as predicted by the auditory CS (Same) and pressing on the other available lever (Different). Virus x Lever x CS period: $F_{(1, 22)} = 4.48$, $P = 0.046$; Lever x CS period: $F_{(1, 22)} = 19.04$, $P = 0.0002$; Lever: $F_{(1, 22)} = 0.001$, $P = 0.97$; Virus: $F_{(1, 22)} = 0.14$, $P = 0.72$; CS period: $F_{(1, 22)} = 7.45$, $P = 0.01$; Virus x Lever: $F_{(1, 22)} = 1.57$, p =0.22; Virus x CS: $F_{(1, 22)} = 1.24$, $P = 0.28$. $^{**}P < 0.01$, planned comparisons CS same presses v. preCS same presses and CS different presses v. preCS different presses. **(i)** Elevation in lever presses on the lever that earned the same outcome as the presented CS (Same; [(Same lever presses during CS)/(Same presses during CS + Same presses during preCS)], averaged across trials and across CSs), relative to the elevation in responding on the alternate lever (Different; [(Different lever presses during CS)/(Different presses during CS + Different presses during preCS)], averaged across trials and across CSs) during the PIT test. Lines represent individual subjects. Virus x Lever: $F_{(1, 22)} = 5.72$, $P = 0.03$; Virus: $F_{(1, 22)} = 3.29$, $P = 0.08$; Lever: $F_{(1, 22)} = 20.82$, $P = 0.0002$. $^{***}P < 0.001$, Bonferroni correction. **(j)** Food-port entry rate during the CS relative to the preCS period, averaged across trials and across the 2 CSs during the PIT test. CS period: $F_{(1, 22)} = 36.10$, $P < 0.0001$; Virus: $F_{(1, 22)} = 0.08$, $P = 0.77$; Virus x CS: $F_{(1, 22)} = 1.65$, $P = 0.21$. $^{**}P < 0.01$, $^{***}P < 0.001$, Bonferroni correction. ChR2, $N = 11$, 6 males; eYFP, $N = 13$, 6 males.

DISCUSSION

Here we reveal the contribution of the VTA_{DA}→BLA pathway to the encoding of detailed, identity-specific, appetitive stimulus-outcome memories. We found that the BLA is active and dopamine is released into the BLA at the time of stimulus-outcome pairing, when subjects have the opportunity to link the features of a rewarding outcome to a predictive cue. Correspondingly, VTA_{DA}→BLA projection activity at stimulus-outcome pairing is necessary to encode identity-specific stimulus-outcome memories, but not to develop a Pavlovian goal-approach response or cache value to the cues to support general motivation. VTA_{DA}→BLA pathway activation is sufficient to rescue the encoding of identity-specific stimulus-outcome memories in a Pavlovian blocking task, but is neither reinforcing itself nor sufficient to enhance reinforcement of a Pavlovian goal-approach response. These data reveal the VTA_{DA}→BLA pathway as a critical contributor to the formation of detailed stimulus-outcome memories, fundamental components of the internal model of environmental relationships, aka cognitive map, that supports flexible decision making.

BLA neuron activity and dopamine release in the BLA is associated with cues and outcomes during Pavlovian conditioning. We detected BLA neuronal and dopamine responses to cue presentation on the first day of training. These responses likely reflect the initial novelty of the stimuli, which habituates in the absence of reward[36, 54-57]. Unlike early in training, later cue-evoked activations result from associative learning[20, 34, 36, 58-64]. Indeed, we continued to find robust BLA and BLA dopamine responses to cue onset throughout training. We also detected BLA neuronal and dopamine responses to cue offset/outcome delivery throughout training. When we separated cue offset from outcome delivery after training we found BLA dopamine responses to both, though smaller dopamine responses to CS offset absent reward. Thus, both BLA neurons and dopamine respond to cues, rewards, and their pairing, when cues can become linked to the identifying features of the outcomes they predict.

VTA_{DA}→BLA pathway activity at the time of stimulus-outcome pairing drives the encoding of identity-specific reward memories. Inhibiting VTA_{DA}→BLA projections at the time of the outcome during Pavlovian conditioning attenuated the ability to link the identifying details of that outcome to the predictive cue such that subjects were unable to later use information about the predicted reward to inform decision making. Stimulation of VTA_{DA}→BLA projections was sufficient to rescue the encoding of identity-specific stimulus-outcome memories, such that subjects were later able to use these memories to inform decision making. Thus, VTA_{DA}→BLA activity is both necessary and sufficient for the formation of detailed reward memories. This is consistent with prior evidence that VTA_{DA} neurons track learning from unexpected changes in outcome identity[65] and can signal the identifying features of an outcome[18]. It also accords with data that VTA_{DA} neuron activity mediates unblocking driven by changes in outcome identity[22] and drives learning about the identifying features of predicted rewards needed for sensitivity of cue responses to outcome-specific devaluation[21]. The present data indicate VTA_{DA} neurons mediate the encoding of identity-specific reward memories and that this is achieved, at least in part, via projections to BLA.

The VTA_{DA}→BLA pathway does not assign general value to cues or mediate reinforcement. The canonical theory of dopamine function is that it provides a teaching signal to cache the general value of future rewarding events to a predictive cue and reinforce response policies based on past success[1-7]. If VTA_{DA}→BLA projections mediate this function, then we should have found their inhibition to disrupt the development of a conditional approach response and prevent cues from supporting general motivated behavior (food-port entries, non-specific lever pressing). To the contrary, conditional food-port approach responses and general cue-induced motivation were preserved following VTA_{DA}→BLA inhibition. This is consistent with evidence that the BLA itself is dispensable for these processes[36, 66, 67]. If VTA_{DA}→BLA pathway activity is sufficient to cache general value to cues and promote reinforcement, then we should have found activation of this pathway to be reinforcing itself, to promote the reinforcement of conditional approach responses, and/or that pairing stimulation with a cue would cause that cue to later promote non-specific motivation. We found no evidence of this. Thus, any contribution of dopamine to general value and reinforcement learning is likely via pathways other than those to the BLA. VTA_{DA}→BLA projections may be specialized for encoding the identity-specific memories that support adaptive decision making.

By establishing a function for the VTA_{DA}→BLA pathway in identity-specific stimulus-outcome memory, these data open new and important questions for future investigation. One is how VTA_{DA}→BLA projections contribute to learning. VTA_{DA} neurons are well known to support learning by signaling errors in reward prediction[1, 3, 6]. VTA_{DA} axons in the BLA can reflect some properties of a prediction error[34], but also show increased activity to both appetitive and aversive events, indicating that they do not strictly encode reward prediction error[34]. Recent evidence indicates that dopamine neurons can support more complex learning by signaling reward identity and even sensory errors[13, 18, 65]. Whether such signals occur

in VTA_{DA}→BLA projections to support stimulus-outcome learning is an interesting possibility. VTA_{DA} neurons can also support learning by signaling perceived salience[68, 69]. VTA_{DA} axons in the BLA can reflect motivational salience[34]. BLA dopamine has also been shown to shape attention-related learning signals in the BLA[70]. The dual reward, long-delay conditioning task, necessary here to probe identity-specific stimulus-outcome memory and its influence on decision making, prevented clean assessment of BLA dopamine encoding of these processes. Thus, whether BLA dopamine supports reward encoding by signaling salience, attention, and/or components of prediction error is a critical open question.

Regarding mechanism, VTA_{DA} projections are positioned to influence stimulus-outcome learning via modulation of neuronal plasticity in the BLA. Dopamine can act on GABAergic interneurons to increase spontaneous inhibitory network activity[34, 71, 72] and enhance long-term potentiation through suppression of feedforward inhibition[73]. Like dopaminergic function in the prefrontal cortex[74, 75], this balance could enhance signal-to-noise by filtering out weak inputs to ensure only strong inputs conveying important information are potentiated. Indeed, dopamine can enhance BLA neuron excitability[71] and activation of VTA_{DA}→BLA projections can elevate the second messenger cyclic adenosine monophosphate and enhance BLA responses to cues[76]. An exciting possibility is that dopamine may gate plasticity in BLA[76-80]. Indeed, dopamine has long been known to modulate synaptic plasticity in striatal circuits[81-83]. Separate populations of BLA neurons can encode unique appetitive outcomes[84, 85]. VTA_{DA}→BLA projections may contribute to identity-specific associative learning by facilitating the formation of these neuronal groups. This is a ripe question for future investigation. Another is the excitatory synapses that dopamine signaling may potentiate. One likely candidate is BLA input from the lateral orbitofrontal cortex, which mediates the encoding of identity-specific reward memories[36]. At least in mice, some VTA_{DA}→BLA projections can corelease glutamate to activate BLA interneurons[34]. That BLA dopamine release coincides with stimulus-outcome pairing suggests dopamine is likely to be involved, but the extent to which glutamate corelease contributes is another important open question.

Findings from this study have important implications for how we conceptualize VTA_{DA} function. They contribute to the emerging understanding that VTA_{DA} neurons have a multifaceted role in learning[25-29]. This and other recent work on more canonical dopamine pathways[21, 86, 87] indicates dopamine's multifaceted contribution to learning is likely dictated by the function of downstream target regions. As we further explore the function of distinct dopamine pathways we may reveal core principles of dopamine function, e.g., learning and/or plasticity modulation, but we will most certainly find diversity of function based on projection target. Here we show that the VTA_{DA}→BLA pathway drives the formation of an association between a cue and the unique outcome it predicts. Such identity-specific stimulus-outcome memories are fundamental components of the internal model of environmental relationships, cognitive map, that enables us to generate the predictions and inferences that support flexible decision making[8, 9, 11, 12]. This core form of memory can support a diverse array of behavioral and decision functions. Thus,

VTA_{DA}→BLA projections may also support identity-specific social, drug, and/or aversive memories. Indeed, VTA_{DA}→BLA projections are involved in aversive learning and behavior[32, 34, 88]. An inability to properly encode predicted outcomes can lead to ill-informed motivations and decisions. This is characteristic of the cognitive symptoms underlying many psychiatric diseases[89-100]. Thus, these data may also aid our understanding and treatment of substance use disorder and mental illnesses marked by disruptions to dopamine function and decision making.

ACKNOWLEDGEMENTS

This research was supported by NIH grant DA035443 and MH106972 (KMW), NSF GRFP (ACS), NSF CAREER 2143910 (MJS), and the Staglin Center for Behavior and Brain Sciences.

AUTHOR CONTRIBUTIONS

KMW and ACS designed the research, analyzed, and interpreted the data. ACS conducted the research with assistance from YXJ. CMG and TMW conducted the behavioral blocking experiments. KR contributed to the fiber photometry experiments. NKG assisted with histological verification. MJS contributed to the design of the blocking experiments, advised on the project, and edited the manuscript. ACS and KMW wrote the manuscript.

COMPETING FINANCIAL INTERESTS

The authors declare no biomedical financial interests or potential conflicts of interest.

REFERENCES

1. Schultz, W., Dayan, P. & Montague, P.R. A neural substrate of prediction and reward. *Science* **275**, 1593-1599 (1997).
2. Waelti, P., Dickinson, A. & Schultz, W. Dopamine responses comply with basic assumptions of formal learning theory. *Nature* **412**, 43-48 (2001).
3. Steinberg, E.E.*, et al.* A causal link between prediction errors, dopamine neurons and learning. *Nat Neurosci* **16**, 966-973 (2013).
4. Schultz, W. Predictive reward signal of dopamine neurons. *J Neurophysiol* **80**, 1-27 (1998).
5. Starkweather, C.K. & Uchida, N. Dopamine signals as temporal difference errors: recent advances. *Curr Opin Neurobiol* **67**, 95-105 (2021).
6. Eshel, N., Tian, J., Bukwich, M. & Uchida, N. Dopamine neurons share common response function for reward prediction error. *Nat Neurosci* **19**, 479-486 (2016).
7. Montague, P.R., Dayan, P. & Sejnowski, T.J. A framework for mesencephalic dopamine systems based on predictive Hebbian learning. *J Neurosci* **16**, 1936-1947 (1996).
8. Delamater, A.R. On the nature of CS and US representations in Pavlovian learning. *Learn Behav* **40**, 1-23 (2012).
9. Fanselow, M.S. & Wassum, K.M. The Origins and Organization of Vertebrate Pavlovian Conditioning. *Cold Spring Harb Perspect Biol* (2015).
10. Tolman, E.C. Cognitive maps in rats and men. *Psychol Rev* **55**, 189-208 (1948).
11. Dayan, P. & Daw, N.D. Decision theory, reinforcement learning, and the brain. *Cogn Affect Behav Neurosci* **8**, 429-453 (2008).
12. Balleine, B.W. The Meaning of Behavior: Discriminating Reflex and Volition in the Brain. *Neuron* **104**, 47-62 (2019).
13. Sharpe, M.J.*, et al.* Dopamine transients are sufficient and necessary for acquisition of model-based associations. *Nature Neuroscience* **20**, 735 (2017).
14. Sharpe, M.J. & Schoenbaum, G. Evaluation of the hypothesis that phasic dopamine constitutes a cached-value signal. *Neurobiology of learning and memory* **153**, 131-136 (2018).
15. Sharpe, M.J.*, et al.* Dopamine transients do not act as model-free prediction errors during associative learning. *Nat Commun* **11**, 106 (2020).
16. Engelhard, B.*, et al.* Specialized coding of sensory, motor and cognitive variables in VTA dopamine neurons. *Nature*, 1 (2019).
17. Sharp, M.E., Foerde, K., Daw, N.D. & Shohamy, D. Dopamine selectively remediates 'model-based'reward learning: a computational approach. *Brain* **139**, 355-364 (2015).
18. Stalnaker, T.*, et al.* Dopamine neuron ensembles signal the content of sensory prediction errors. *BioRxiv*, 723908 (2019).
19. Howard, J.D. & Kahnt, T. Identity prediction errors in the human midbrain update reward-identity expectations in the orbitofrontal cortex. *Nature communications* **9**, 1611 (2018).
20. Sadacca, B.F., Jones, J.L. & Schoenbaum, G. Midbrain dopamine neurons compute inferred and cached value prediction errors in a common framework. *Elife* **5** (2016).
21. Keiflin, R., Pribut, H.J., Shah, N.B. & Janak, P.H. Ventral Tegmental Dopamine Neurons Participate in Reward Identity Predictions. *Curr Biol* **29**, 93-103.e103 (2019).
22. Chang, C.Y., Gardner, M., Di Tillio, M.G. & Schoenbaum, G. Optogenetic Blockade of Dopamine Transients Prevents Learning Induced by Changes in Reward Features. *Curr Biol* **27**, 3480-3486.e3483 (2017).
23. Wunderlich, K., Smittenaar, P. & Dolan, R.J. Dopamine enhances model-based over model-free choice behavior. *Neuron* **75**, 418-424 (2012).
24. Seitz, B.M., Hoang, I.B., DiFazio, L.E., Blaisdell, A.P. & Sharpe, M.J. Dopamine errors drive excitatory and inhibitory components of backward conditioning in an outcome-specific manner. *Curr Biol* **32**, 3210-3218.e3213 (2022).
25. Langdon, A.J., Sharpe, M.J., Schoenbaum, G. & Niv, Y. Model-based predictions for dopamine. *Curr Opin Neurobiol* **49**, 1-7 (2018).
26. Gardner, M.P.H., Schoenbaum, G. & Gershman, S.J. Rethinking dopamine as generalized prediction error. *Proc Biol Sci* **285** (2018).
27. Nasser, H.M., Calu, D.J., Schoenbaum, G. & Sharpe, M.J. The Dopamine Prediction Error: Contributions to Associative Models of Reward Learning. *Front Psychol* **8**, 244 (2017).
28. Keiflin, R. & Janak, P.H. Error-Driven Learning: Dopamine Signals More Than Value-Based Errors. *Curr Biol* **27**, R1321-R1324 (2017).
29. Seitz, B.M., Blaisdell, A.P. & Sharpe, M.J. Higher-Order Conditioning and Dopamine: Charting a Path Forward. *Front Behav Neurosci* **15**, 745388 (2021).
30. Brinley-Reed, M. & McDonald, A.J. Evidence that dopaminergic axons provide a dense innervation of specific neuronal subpopulations in the rat basolateral amygdala. *Brain Res* **850**, 127-135 (1999).
31. Fallon, J. & Ciofi, P. Distribution of monoamines within the amygdala. in *The Amygdala* (ed. J. Aggleton) 97-114 (Academic Press, New York, 1992).
32. Tang, W., Kochubey, O., Kintscher, M. & Schneggenburger, R. A VTA to Basal Amygdala Dopamine Projection Contributes to Signal Salient Somatosensory Events during Fear Learning. *J Neurosci* **40**, 3969-3980 (2020).
33. Sadikot, A.F. & Parent, A. The monoaminergic innervation of the amygdala in the squirrel monkey: an immunohistochemical study. *Neuroscience* **36**, 431-447 (1990).
34. Lutas, A.*, et al.* State-specific gating of salient cues by midbrain dopaminergic input to basal amygdala. *Nat Neurosci* **22**, 1820-1833 (2019).

35. Beier, K.T., *et al.* Circuit Architecture of VTA Dopamine Neurons Revealed by Systematic Input-Output Mapping. *Cell* **162**, 622-634 (2015).
36. Sias, A., *et al.* A bidirectional corticoamygdala circuit for the encoding and retrieval of detailed reward memories. *eLife* **10** (2021).
37. Chen, T.W., *et al.* Ultrasensitive fluorescent proteins for imaging neuronal activity. *Nature* **499**, 295-300 (2013).
38. Delamater, A. Effects of several extinction treatments upon the integrity of Pavlovian stimulus-outcome associations. *Animal Learning & Behavior* **24**, 437-739 (1996).
39. Colwill, R.M. & Motzkin, D.K. Encoding of the unconditioned stimulus in Pavlovian conditioning. *Animal Learning & Behavior* **22**, 384-394 (1994).
40. Rescorla, R. Learning about qualitatively different outcomes during a blocking procedure. *Animal Learning & Behavior* **27**, 140-151 (1999).
41. Delamater, A.R. & Holland, P.C. The influence of CS-US interval on several different indices of learning in appetitive conditioning. *J Exp Psychol Anim Behav Process* **34**, 202-222 (2008).
42. Rescorla, R.A. Retraining of extinguished Pavlovian stimuli. *J Exp Psychol Anim Behav Process* **27**, 115-124 (2001).
43. RA, R. Preservation of Pavlovian associations through extinction. *The Quarterly Journal of Experimental Psychology: Section B* **49.3**, 245-258 (1996).
44. Paxinos, G. & Watson, C. *The rat brain in stereotaxic coordinates* (Academic Press, 1998).
45. Sun, F., *et al.* Next-generation GRAB sensors for monitoring dopaminergic activity in vivo. *Nat Methods* **17**, 1156-1166 (2020).
46. Witten, I.B., *et al.* Recombinase-driver rat lines: tools, techniques, and optogenetic application to dopamine-mediated reinforcement. *Neuron* **72**, 721-733 (2011).
47. Kruse, H., Overmier, J., Konz, W. & Rokke, E. Pavlovian conditioned stimulus effects upon instrumental choice behavior are reinforcer specific. *Learn Motiv* **14**, 165-181 (1983).
48. Corbit, L.H. & Balleine, B.W. Learning and Motivational Processes Contributing to Pavlovian-Instrumental Transfer and Their Neural Bases: Dopamine and Beyond. *Curr Top Behav Neurosci* (2016).
49. Kamin, L. Predictability, surprise, attention, and conditioning. in *SYMP. ON PUNISHMENT* (1967).
50. Kamin, L.J. "Attention-like" processes in classical conditioning. in *Miami symposium on the prediction of behavior: aversive stimulation* 9-31 (University of Miami Press, Miami, 1968).
51. Kamin, L.J. Selective association and conditioning. in *Fundamental Issues in Instrumental Learning* (ed. N.J. Mackintosh & W.K. Honig) 42-64 (Dalhousie University Press, Halifax, 1969).
52. Rescorla, R.A. Learning about qualitatively different outcomes during a blocking procedure. *Animal Learning & Behavior* **27**, 140-151 (1999).
53. Coddington, L.T. & Dudman, J.T. The timing of action determines reward prediction signals in identified midbrain dopamine neurons. *Nat Neurosci* **21**, 1563-1573 (2018).
54. Ljungberg, T., Apicella, P. & Schultz, W. Responses of monkey dopamine neurons during learning of behavioral reactions. *J Neurophysiol* **67**, 145-163 (1992).
55. Bordi, F. & LeDoux, J. Sensory tuning beyond the sensory system: an initial analysis of auditory response properties of neurons in the lateral amygdaloid nucleus and overlying areas of the striatum. *J Neurosci* **12**, 2493-2503 (1992).
56. Bordi, F., LeDoux, J., Clugnet, M.C. & Pavlides, C. Single-unit activity in the lateral nucleus of the amygdala and overlying areas of the striatum in freely behaving rats: rates, discharge patterns, and responses to acoustic stimuli. *Behav Neurosci* **107**, 757-769 (1993).
57. Bunzeck, N. & Düzel, E. Absolute coding of stimulus novelty in the human substantia nigra/VTA. *Neuron* **51**, 369-379 (2006).
58. Muramoto, K., Ono, T., Nishijo, H. & Fukuda, M. Rat amygdaloid neuron responses during auditory discrimination. *Neuroscience* **52**, 621-636 (1993).
59. Paton, J.J., Belova, M.A., Morrison, S.E. & Salzman, C.D. The primate amygdala represents the positive and negative value of visual stimuli during learning. *Nature* **439**, 865-870 (2006).
60. Saddoris, M.P., Gallagher, M. & Schoenbaum, G. Rapid associative encoding in basolateral amygdala depends on connections with orbitofrontal cortex. *Neuron* **46**, 321-331 (2005).
61. Schoenbaum, G., Chiba, A.A. & Gallagher, M. Neural encoding in orbitofrontal cortex and basolateral amygdala during olfactory discrimination learning. *J Neurosci* **19**, 1876-1884 (1999).
62. Day, J.J., Roitman, M.F., Wightman, R.M. & Carelli, R.M. Associative learning mediates dynamic shifts in dopamine signaling in the nucleus accumbens. *Nat Neurosci* **10**, 1020-1028 (2007).
63. Schultz, W., Dayan, P. & Montague, P.R. A neural substrate of prediction and reward. *Science* **275**, 1593-1599 (1997).
64. Cone, J.J., *et al.* Physiological state gates acquisition and expression of mesolimbic reward prediction signals. *Proc Natl Acad Sci U S A* **113**, 1943-1948 (2016).
65. Takahashi, Y.K., *et al.* Dopamine Neurons Respond to Errors in the Prediction of Sensory Features of Expected Rewards. *Neuron* **95**, 1395-1405.e1393 (2017).
66. Hatfield, T., Han, J.S., Conley, M., Gallagher, M. & Holland, P. Neurotoxic lesions of basolateral, but not central, amygdala interfere with Pavlovian second-order conditioning and reinforcer devaluation effects. *J Neurosci* **16**, 5256-5265 (1996).
67. Corbit, L.H. & Balleine, B.W. Double dissociation of basolateral and central amygdala lesions on the general and outcome-specific forms of pavlovian-instrumental transfer. *J Neurosci* **25**, 962-970 (2005).
68. Kutlu, M.G., *et al.* Dopamine release in the nucleus accumbens core signals perceived saliency. *Curr Biol* **31**, 4748-4761.e4748 (2021).

69. Kutlu, M.G., *et al.* Dopamine signaling in the nucleus accumbens core mediates latent inhibition. *Nat Neurosci* **25**, 1071-1081 (2022).
70. Esber, G.R., *et al.* Attention-related Pearce-Kaye-Hall signals in basolateral amygdala require the midbrain dopaminergic system. *Biol Psychiatry* **72**, 1012-1019 (2012).
71. Kröner, S., Rosenkranz, J.A., Grace, A.A. & Barrionuevo, G. Dopamine modulates excitability of basolateral amygdala neurons in vitro. *J Neurophysiol* **93**, 1598-1610 (2005).
72. Lorétan, K., Bissière, S. & Lüthi, A. Dopaminergic modulation of spontaneous inhibitory network activity in the lateral amygdala. *Neuropharmacology* **47**, 631-639 (2004).
73. Bissière, S., Humeau, Y. & Lüthi, A. Dopamine gates LTP induction in lateral amygdala by suppressing feedforward inhibition. *Nat Neurosci* **6**, 587-592 (2003).
74. Vander Weele, C.M., *et al.* Dopamine enhances signal-to-noise ratio in cortical-brainstem encoding of aversive stimuli. *Nature* **563**, 397-401 (2018).
75. Stalter, M., Westendorff, S. & Nieder, A. Dopamine Gates Visual Signals in Monkey Prefrontal Cortex Neurons. *Cell Rep* **30**, 164-172.e164 (2020).
76. Lutas, A., Fernando, K., Zhang, S.X., Sambangi, A. & Andermann, M.L. History-dependent dopamine release increases cAMP levels in most basal amygdala glutamatergic neurons to control learning. *Cell Rep* **38**, 110297 (2022).
77. Rosenkranz, J.A. & Grace, A.A. Cellular mechanisms of infralimbic and prelimbic prefrontal cortical inhibition and dopaminergic modulation of basolateral amygdala neurons in vivo. *J Neurosci* **22**, 324-337 (2002).
78. Rosenkranz, J.A. & Grace, A.A. Dopamine-mediated modulation of odour-evoked amygdala potentials during pavlovian conditioning. *Nature* **417**, 282-287 (2002).
79. Li, C. & Rainnie, D.G. Bidirectional regulation of synaptic plasticity in the basolateral amygdala induced by the D1-like family of dopamine receptors and group II metabotropic glutamate receptors. *J Physiol* **592**, 4329-4351 (2014).
80. Li, C., Dabrowska, J., Hazra, R. & Rainnie, D.G. Synergistic activation of dopamine D1 and TrkB receptors mediate gain control of synaptic plasticity in the basolateral amygdala. *PLoS One* **6**, e26065 (2011).
81. Speranza, L., di Porzio, U., Viggiano, D., de Donato, A. & Volpicelli, F. Dopamine: The Neuromodulator of Long-Term Synaptic Plasticity, Reward and Movement Control. *Cells* **10** (2021).
82. Calabresi, P., Picconi, B., Tozzi, A. & Di Filippo, M. Dopamine-mediated regulation of corticostriatal synaptic plasticity. *Trends Neurosci* **30**, 211-219 (2007).
83. Reynolds, J.N. & Wickens, J.R. Dopamine-dependent plasticity of corticostriatal synapses. *Neural Netw* **15**, 507-521 (2002).
84. Liu, J., *et al.* Neural Coding of Appetitive Food Experiences in the Amygdala. *Neurobiol Learn Mem* **155**, 261-275 (2018).
85. Courtin, J., *et al.* A neuronal mechanism for motivational control of behavior. *Science* **375**, eabg7277 (2022).
86. Collins, A.L. & Saunders, B.T. Heterogeneity in striatal dopamine circuits: Form and function in dynamic reward seeking. *J Neurosci Res* **98**, 1046-1069 (2020).
87. Saunders, B.T., Richard, J.M., Margolis, E.B. & Janak, P.H. Dopamine neurons create Pavlovian conditioned stimuli with circuit-defined motivational properties. *Nat Neurosci* **21**, 1072-1083 (2018).
88. Morel, C., *et al.* Midbrain projection to the basolateral amygdala encodes anxiety-like but not depression-like behaviors. *Nat Commun* **13**, 1532 (2022).
89. Hogarth, L., Balleine, B.W., Corbit, L.H. & Killcross, S. Associative learning mechanisms underpinning the transition from recreational drug use to addiction. *Ann N Y Acad Sci* **1282**, 12-24 (2013).
90. Morris, R.W., Quail, S., Griffiths, K.R., Green, M.J. & Balleine, B.W. Corticostriatal control of goal-directed action is impaired in schizophrenia. *Biol Psychiatry* **77**, 187-195 (2015).
91. Seymour, B. & Dolan, R. Emotion, decision making, and the amygdala. *Neuron* **58**, 662-671 (2008).
92. Alvares, G.A., Balleine, B.W. & Guastella, A.J. Impairments in goal-directed actions predict treatment response to cognitive-behavioral therapy in social anxiety disorder. *PLoS One* **9**, e94778 (2014).
93. Gleichgerrcht, E., Ibáñez, A., Roca, M., Torralva, T. & Manes, F. Decision-making cognition in neurodegenerative diseases. *Nat Rev Neurol* **6**, 611-623 (2010).
94. Hogarth, L., Balleine, B.W., Corbit, L.H. & Killcross, S. Associative learning mechanisms underpinning the transition from recreational drug use to addiction. *Ann N Y Acad Sci* (2012).
95. Dayan, P. Dopamine, reinforcement learning, and addiction. *Pharmacopsychiatry* **42 Suppl 1**, S56-65 (2009).
96. Voon, V., *et al.* Disorders of compulsivity: a common bias towards learning habits. *Mol Psychiatry* **20**, 345-352 (2015).
97. Heller, A.S., Ezie, C.E.C., Otto, A.R. & Timpano, K.R. Model-based learning and individual differences in depression: The moderating role of stress. *Behav Res Ther* **111**, 19-26 (2018).
98. Chen, C., Takahashi, T., Nakagawa, S., Inoue, T. & Kusumi, I. Reinforcement learning in depression: A review of computational research. *Neurosci Biobehav Rev* **55**, 247-267 (2015).
99. Huys, Q.J., Daw, N.D. & Dayan, P. Depression: a decision-theoretic analysis. *Annu Rev Neurosci* **38**, 1-23 (2015).
100. Culbreth, A.J., Westbrook, A., Daw, N.D., Botvinick, M. & Barch, D.M. Reduced model-based decision-making in schizophrenia. *J Abnorm Psychol* **125**, 777-787 (2016).
101. Collins, A.L., *et al.* Nucleus Accumbens Cholinergic Interneurons Oppose Cue-Motivated Behavior. *Biol Psychiatry* (2019).
102. Malvaez, M., Shieh, C., Murphy, M.D., Greenfield, V.Y. & Wassum, K.M. Distinct cortical–amygdala projections drive reward value encoding and retrieval. *Nature Neuroscience* (2019).
103. Lichtenberg, N.T., *et al.* The medial orbitofrontal cortex - basolateral amygdala circuit regulates the influence of reward cues on adaptive behavior and choice. *J Neurosci* (2021).

104. Malvaez, M.*, et al.* Basolateral amygdala rapid glutamate release encodes an outcome-specific representation vital for reward-predictive cues to selectively invigorate reward-seeking actions. *Sci Rep* **5**, 12511 (2015).
105. Lopes, G.*, et al.* Bonsai: an event-based framework for processing and controlling data streams. *Front Neuroinform* **9**, 7 (2015).
106. Schmider, E., Ziegler, M., Danay, E., Beyer, L. & Bühner, M. Is it really robust? Reinvestigating the robustness of ANOVA against violations of the normal distribution assumption. *Methodology : European journal of research methods for the behavioral & social sciences* **6**, 147-151 (2010).
107. Knief, U. & Forstmeier, W. Violating the normality assumption may be the lesser of two evils. *Behav Res Methods* **53**, 2576-2590 (2021).
108. Levin, J.R., Serlin, R.C., Seaman & M.A. A controlled powerful multiple-comparison strategy for several situations . *Psychological Bulletin* **115**, 153-159 (1994).
109. Lichtenberg, N.T. & Wassum, K.M. Amygdala mu-opioid receptors mediate the motivating influence of cue-triggered reward expectations. *Eur J Neurosci* (2016).
110. Lichtenberg, N.T.*, et al.* Basolateral amygdala to orbitofrontal cortex projections enable cue-triggered reward expectations. *J Neurosci* (2017).

METHODS

Subjects

Male and female wildtype Long-Evans rats and transgenic Long-Evans rats expressing Cre recombinase under control of the tyrosine hydroxylase (Th) promoter (Th-cre) aged 8 - 11 weeks at the time of surgery served as subjects. Rats were housed in a temperature (68-79°F) and humidity (30-70%) regulated vivarium. They were initially housed in same-sex pairs and then following surgery housed individually to preserve implants. Rats were provided with water *ad libitum* in the home cage and were maintained on a food-restricted 12-14 g daily diet (Lab Diet, St. Louis, MO) to maintain approximately 85-90% free-feeding body weight. Rats were handled for 3-5 days prior to the onset of each experiment. Separate groups of naïve rats were used for each experiment. Experiments were performed during the dark phase of a 12:12 hr reverse dark/light cycle (lights off at 7AM). All procedures were conducted in accordance with the NIH Guide for the Care and Use of Laboratory Animals and were approved by the UCLA Institutional Animal Care and Use Committee.

Surgery

We used standard surgical procedures described previously[36, 101-103]. Rats were anesthetized with isoflurane (4–5% induction, 1–2% maintenance), and a nonsteroidal anti-inflammatory agent was administered pre- and postoperatively to minimize pain and discomfort. Surgical details for each experiment are described below. In all cases, surgery occurred prior to the onset of behavioral training.

Behavioral procedures

Apparatus

Training took place in Med Associates conditioning chambers (East Fairfield, VT) housed within sound- and light-attenuating boxes, described previously[104]. Each chamber had grid floors and contained 2 retractable levers that could be inserted to the left and right of a recessed food-delivery port (magazine) on the front wall. Stimulus lights were positioned above each of these levers. A photobeam entry detector was positioned at the entry to the food port. Each chamber was equipped with a syringe pump to deliver 20% sucrose solution in 0.1 ml increments through a stainless-steel tube into one well of the food port and a pellet dispenser to deliver 45-mg grain pellets (Bio-Serv, Frenchtown, NJ) into another well of the same port. A white noise generator was attached to a speaker on the wall opposite the levers and food-delivery port. A clicker was also mounted on this wall. A fan mounted to the outer chamber provided ventilation and external noise reduction. A 3-watt, 24-volt house light mounted on the top of the back wall opposite the food port provided illumination, except in Pavlovian blocking experiments for which it was used as a conditioned stimulus. For the Pavlovian blocking behavioral experiment, two stimulus lights were also positioned facing up outside, but immediately adjacent to the chamber at floor level on the front left corner and back right corner. Chambers used for intracranial self-stimulation contained 2 nose poke ports on the wall with the house light, a smooth plexiglass floor, and rounded wall opposite the nose pokes. They did not contain levers or food-delivery port. For optogenetic manipulations, chambers were outfitted with an Intensity Division Fiberoptic Rotary Joint (Doric Lenses, Quebec, QC, Canada)

connecting the output fiber optic patch cords to a laser (Dragon Lasers, ChangChun, JiLin, China) positioned outside of the chamber.

Pavlovian conditioning

Magazine conditioning. Rats first received 2 days of training to learn where to receive the sucrose (20%, 0.1 ml/delivery) and food pellet (45 mg grain; Bio-Serv) outcomes. Each day included 2 sessions, separated by approximately 1 hr, order counterbalanced across days, one with 30 non-contingent deliveries of sucrose and one with 30 grain pellet deliveries (60-s intertrial interval, ITI).

Preexposure. To reduce the initial saliency of the auditory stimuli used in subsequent Pavlovian conditioning, subjects received one day of preexposure to the click and white noise stimuli. Click and noise were presented pseudo-randomly for 30-s durations, 4 times each with a variable 1.5 – 3-min ITI (mean = 2.5 min).

Pavlovian conditioning. All rats received 8 sessions of Pavlovian conditioning (1 session/day on consecutive days) to learn to associate each of 2 auditory conditioned stimuli (CSs; 80-82 db), click (10 Hz) and white noise, with a specific food outcome, sucrose solution or grain pellets. Each 30-s CS terminated with the delivery of its associated outcome. For half the subjects, click terminated in the delivery of sucrose and noise predicted pellets, with the other half receiving the opposite arrangement. Each session consisted of 8 click and 8 white noise presentations. CSs were delivered pseudo-randomly with a variable 1.5 – 3-min ITI (mean = 2.5 min).

Pavlovian-to-instrumental transfer

Magazine conditioning. Rats first received 2 days of training to learn where to receive the sucrose (20%, 0.1 ml/delivery) and food pellet (45 mg grain; Bio-Serv) outcomes. Each day included 2 sessions, separated by approximately 1 hr, order counterbalanced across days, one with 30 non-contingent deliveries of sucrose and one with 30 grain pellet deliveries (60-s ITI).

Instrumental conditioning. Rats next received 11 days, minimum, of instrumental conditioning. They received 2 training sessions per day, one with the left lever and one with the right lever, separated by at least 1 hr with order alternated across days. Each action was reinforced with one of the different food outcomes (e.g., left press→grain pellets/right press→sucrose solution). Lever-outcome pairings were counterbalanced at the start of the experiment within each group. Each session terminated after 20 outcomes had been earned or 45 min had elapsed. Actions were continuously reinforced on the first day and then escalated ultimately to a random-ratio (RR) 20 schedule of reinforcement in which a variable number of presses (average = 20) were required to earn a reward.

Pavlovian conditioning. All rats received 8 sessions of Pavlovian conditioning (1 session/day on consecutive days) to learn to associate each of 2 auditory conditioned stimuli (CSs; 80-82 db), click (10 Hz) and white noise, with a specific food outcome, sucrose solution or grain pellets. Each 30-s CS terminated with the delivery of its associated outcome. For half the subjects, click terminated in the delivery of sucrose and noise predicted pellets, with the other half receiving the opposite arrangement. CS-outcome pairings were counterbalanced within groups and with respect to instrumental lever-outcome pairings. Each session consisted of 8 click and 8 white noise presentations. CSs were delivered pseudo-randomly with a variable 1.5 – 3-min ITI (mean = 2.5 min).

Instrumental retraining and extinction. Following Pavlovian conditioning, rats received one day of instrumental retraining on the RR-20 reinforcement schedule. Rats then received one day of instrumental extinction to establish a low level of pressing. During this single 30-min session both levers were available but pressing was not reinforced.

Outcome-specific Pavlovian-to-instrumental transfer tests. Rats next received an outcome-specific Pavlovian-to-instrumental transfer (PIT) test. During the PIT test, both levers were continuously present, but pressing was not reinforced. After 5 min of lever-pressing extinction, each 30-s CS was presented separately 4 times, separated by a fixed 2.5-min ITI, in alternating order. CS order was counterbalanced across subjects. No outcomes were delivered following CS presentation. Rats next received two days of instrumental retraining. This was followed by one day of Pavlovian retraining. After retraining, rats were

given a second PIT test. This test was identical to the first except the pre-extinction phase was 10 min and each rat received the CSs in opposite order to the first test.

Outcome-specific blocking and Pavlovian-to-instrumental transfer

Magazine conditioning. Rats first received 2 days of training to learn where to receive the sucrose (20%, 0.1 ml/delivery) and food pellet (45 mg grain; Bio-Serv) outcomes. Each day included 2 sessions, separated by approximately 1 hr, order counterbalanced across days, one with 30 non-contingent deliveries of sucrose and one with 30 grain pellet deliveries (60-s ITI). The house light was off during these sessions.

Instrumental conditioning. Rats next received 11 days, minimum, of instrumental conditioning. They received 2 separate training sessions per day, one with the left lever and one with the right lever, separated by at least 1 hr with order alternated across days. Each action was reinforced with one of the different food outcomes (e.g., left press→grain pellets/right press→sucrose solution). Lever-outcome pairings were counterbalanced at the start of the experiment within each group. Each session terminated after 20 outcomes had been earned or 45 min had elapsed. Actions were continuously reinforced on the first day and then escalated ultimately to a RR-20 schedule of reinforcement. The house light was off during these sessions.

Pavlovian conditioning. Rats received 12 sessions of visual cue Pavlovian conditioning (1 session/day on consecutive days) in a dark operant chamber to learn to associate visual cues with the food outcomes. For rats in the blocking group, each of 2 30-s duration visual CSs, house light or flashing stimulus lights (2 hz), was paired with a specific food outcome, sucrose (20%, 0.1 ml/delivery) or grain pellets (45 mg; Bio-Serv; e.g., house light—sucrose/flashing light—pellet) CS-outcome pairings were counterbalanced within groups and with respect to instrumental lever-outcome pairings. For half the subjects, the house light terminated in the delivery of sucrose and flashing lights predicted pellets, with the other half receiving the opposite arrangement. Each session consisted of 16 house light and 16 flashing light presentations. CSs were delivered pseudo-randomly with a variable 1.5 – 3-min ITI (mean = 2.5 min). Subjects in the control group (behavioral experiment only) were trained to associate a third distinct, 30-s visual stimulus with both food outcomes. Each session consisted of 32 presentations of lights on either side of the outside of the chamber alternating every 2 s (30-s duration; variable 1.5 – 3-min ITI, mean = 2.5 min). On half the trials the 30-s outside light CS terminated in the delivery of sucrose (20%, 0.1 ml/delivery) and on the other half in in grain pellets (45 mg; Bio-Serv) in pseudorandom order.

Instrumental retraining and extinction. Following Pavlovian conditioning, rats received one day of instrumental retraining on the RR-20 reinforcement schedule. Rats then received one day of instrumental extinction to establish a low level of pressing. During this single 30-min session both levers were available but pressing was not reinforced.

Preexposure. Rats received one day of preexposure to the auditory stimuli. Click and noise were independently presented pseudo-randomly for 30-s durations, 8 times each with a variable 1.5 – 3-min ITI (mean = 2.5 min).

Compound conditioning. Rats next received 4 days of compound conditioning in which the house light and flashing stimulus light CSs were each presented in compound with a distinct auditory stimulus, click (10 Hz) or white noise (80-82 dB). For half the subjects in each group, the house light was presented simultaneously for 30 s with the click and the flashing lights concurrent noise for 30 s. The other half of subjects received the opposite arrangement. Visual-auditory CS pairings were counterbalanced within groups and with respect to instrumental and visual CS-outcome contingencies. For subjects in the blocking group, each compound stimulus terminated in the outcome paired with the visual stimulus during initial Pavlovian conditioning (e.g., house light + white noise—sucrose/flashing light + clicker—pellet). Compound stimulus-outcome pairings were counterbalanced across subjects in the control group. Each compound conditioning session consisted of 8, 30-s presentations of each compound stimulus, terminating in the delivery of the associated food outcome. Compound stimuli were delivered pseudo-randomly with a variable 1.5 – 3-min ITI (mean = 2.5 min).

Outcome-specific Pavlovian-to-instrumental transfer tests. Rats next received an outcome-specific PIT test. During the PIT test, both levers were continuously present, but pressing was not reinforced. After 5 min of lever-pressing extinction, each 30-s CS was presented separately 4 times, separated by a fixed 2.5-min ITI, in alternating order. CS order was counterbalanced across subjects. No outcomes were delivered following CS presentation. The house light was off at test. Rats in the behavioral experiment next received two days of instrumental retraining, one day of Pavlovian retraining with only visual CS presentations and one day of compound retraining prior to a second PIT test. This test was identical to the first except the pre-extinction phase was 10 min and each rat received the CSs in opposite order to the first test.

Data collection

Discrete entries into the food-delivery port and/or lever presses were recorded continuously for each session. For Pavlovian training and PIT test sessions, the 30-s periods prior to each CS onset served as the baseline for comparison of CS-induced changes in lever pressing and/or food-port entries.

Fiber photometry recordings of calcium activity in BLA neurons during Pavlovian conditioning

Subjects

Eight male (*N* = 4) and female (*N* = 4) wildtype rats (Charles River Laboratories, Wilmington, MA) aged approximately 9 weeks at the time of surgery were included in this study to assess BLA neuronal activity changes across Pavlovian conditioning. No subjects were excluded.

Surgery

Rats were infused bilaterally with adeno-associated virus (AAV) expressing the genetically encoded calcium indicator GCaMP6f under control of the calcium/calmodulin-dependent protein kinase (CaMKII) promoter (pENN.AAV5.CAMKII.GCaMP6f.WPRE.SV40, Addgene, Watertown, MA). Virus (0.5 µl) was bilaterally infused into the BLA (AP: -2.9; ML: ± 5.0; DV: -8.8 mm from bregma) at a rate of 0.1 µl/min using 28-gauge injectors. Injectors were left in place for 10 additional min following infusion. Optical fibers (200-µm diameter, 0.37 numerical aperture (NA), Neurophotometrics, San Diego, CA) were implanted bilaterally 0.2 mm dorsal to the infusion site. Experiments commenced approximately 4 weeks after surgery to allow sufficient expression in BLA cell bodies.

Fiber photometry recordings

Animals were habituated to the optical tether during the magazine conditioning sessions, but no light was delivered. Following magazine training, fiber photometry was used to image bulk calcium activity in BLA neurons throughout each Pavlovian conditioning session. We simultaneously imaged GCaMP6f and control fluorescence in the BLA using a commercial fiber photometry system (Neurophotometrics Ltd.). Two light-emitting LEDs (470 nm: Ca2+-dependent GCaMP fluorescence; 415 nm: autofluorescence, motion artifact, Ca2+-independent GCaMP fluorescence) were reflected off dichroic mirrors and coupled via a patch cord (fiber core diameter: 200 µm; Doric Lenses, Quebec, Canada) to the implanted optical fiber. The intensity of excitation light was adjusted to ~80 µW at the tip of the patch cord. Fluorescence emission was passed through a 535 nm bandpass filter and focused onto the complementary metal-oxide semiconductor (CMOS) camera sensor through a tube lens. Samples were collected at 20 Hz interleaved between the 415 nm and 470 nm excitation channels using a custom Bonsai[105] workflow. Time stamps of task events were collected simultaneously through an additional synchronized camera aimed at the Med Associates interface, which sent light pulses coincident with task events. Signals were saved using Bonsai software and exported to MATLAB (MathWorks, Natick, MA) for analysis. Recordings were collected unilaterally from the hemisphere with the strongest fluorescence signal in the 470 nm channel at the start of the experiment.

Fiber photometry recordings of dopamine release in the BLA during Pavlovian conditioning

Subjects

Nine male (*N* = 5) and female (*N* = 4) Long Evans rats (Th-cre- littermates, *N* = 6; Charles River Laboratories, *N* = 3) aged 9-11 weeks at the time of surgery were used to record dopamine release in the BLA across Pavlovian conditioning. Two subjects were excluded from the dataset prior to analysis

for lacking fiber photometry GrabDA2h signal of sufficient quality. An additional 7 subjects were included in a control experiment assessing dopamine release (GrabDA2h; *N* = 4, 3 male) and control GFP fluorescence (*N* = 3, 2 male) during the last Pavlovian conditioning session.

Surgery

Rats were infused bilaterally with AAV encoding the GPCR-activation-based dopamine sensor GRABDA2h (pAAV9-hsyn-GRAB_DA2h, Addgene) or control fluorophore (AAV8-hSYN-GFP). Virus (0.3 µl) was infused bilaterally into the BLA (AP: -2.7; ML: ±5.0; DV: -8.7 males or -8.6 mm females, from bregma). 5 min later, viral injectors were dorsally repositioned in the BLA for a second viral infusion (0.3 µl; DV: -8.4 males or -8.3 mm females). Subjects included in the control experiment received a single viral infusion (0.5 µl; DV: -8.6 mm). Optical fibers (400-µm diameter, 0.37 NA, Neurophotometrics) were implanted bilaterally 0.2 mm dorsal to the first infusion site. Virus was infused at a rate of 0.1 µl/min using 28-gauge injectors and injectors were left in place for 10 min after the second infusion. Experiments commenced approximately 4 weeks after surgery to allow sufficient expression in the BLA.

Fiber photometry recordings

Animals were habituated to the optical tether during the magazine conditioning sessions, but no light was delivered. Following magazine training, fiber photometry was used to image GrabDA2h activity in BLA neurons throughout each Pavlovian conditioning session (*N* = 9) or only during the last (8^{th}) Pavlovian conditioning session (*N* = 4 GrabDA2h, *N* = 3 GFP) using a commercial fiber photometry system (Neurophotometrics Ltd.). 470 nm excitation light was adjusted to approximately 80-100 µW at the tip of the patch cord (fiber core diameter: 400 µm; Doric Lenses) and samples were collected at 20 Hz. Recordings were collected unilaterally from the hemisphere with the strongest fluorescence signal at the start of the experiment.

Optogenetic inhibition of VTA_{DA}→BLA terminals during Pavlovian conditioning

Subjects

Twenty-one male (*N* = 11) and female (*N* = 10) transgenic Th-cre+ (hemizygous) Long Evans rats aged approximately 10 weeks at the time of surgery were used in this study to assess the necessity of VTA_{DA}→BLA projection activity for stimulus-outcome learning. Three subjects with misplaced optic fibers were excluded from the dataset.

Surgery

Th-cre rats were randomly assigned to a viral group and infused bilaterally with a cre-dependent AAV encoding either the inhibitory opsin archaerhodopsin T (ArchT; *N* = 11; 6 males; AAV5-CAG-FLEX-ArchT-tdTomato, Addgene) or a tdTomato fluorescent protein control (tdTomato; *N* = 10; 5 males; AAV5-CAG-FLEX-tdTomato, University of North Carolina Vector Core, Chapel Hill, NC). Virus (0.2 µl) was infused bilaterally at a rate of 0.1 µl/min into the VTA (AP: -5.3; ML: ±0.7; DV: -8.3 mm from bregma) using a 28-gauge injector. Injectors were left in place for 10 min following infusion. Optical fibers (200-µm core, 0.39 NA, Thorlabs, Newton, NJ) held in ceramic ferrules (Kientec Systems, Stuart, FL) were implanted bilaterally in the BLA (AP: -2.7; ML: ±5.0; DV: -8.2 mm from bregma). Experiments commenced 4-5 weeks after surgery to allow sufficient expression in VTA_{DA}→BLA terminals at the time of manipulation (7-9 weeks after surgery).

Optogenetic inhibition of VTA_{DA}→BLA projections

Rats received magazine and instrumental training as above. Animals were habituated to the optical tether (200 µm, 0.22 NA, Doric Lenses) for at least the last 2 days of instrumental conditioning, but no light was delivered. Optogenetic inhibition was used to attenuate the activity of ArchT-expressing VTA_{DA} axons and terminals in the BLA at the time of stimulus-outcome pairing during each Pavlovian conditioning session. During each Pavlovian conditioning session, green light (532 nm; 10 mW) was delivered to the BLA via a laser (Dragon Lasers) connected through a ceramic mating sleeve (Thorlabs) to the ferrule implanted on the rat. Light was delivered continuously for 3 s concurrent with each outcome delivery (occurring at CS offset). If the outcome was retrieved after the laser had gone off, then the retrieval entry (first food-port entry after outcome delivery) triggered an additional 3-s illumination. Light effects were

estimated to be restricted to the BLA based on predicted irradiance values (https://web.stanford.edu/group/dlab/cgi-bin/graph/chart.php). Following Pavlovian conditioning, rats proceeded to the PIT tests as described above, during which they were tethered to the optical patch cords, but no light was delivered. The same light delivery procedures were used during Pavlovian retraining in between PIT tests.

Outcome-specific Pavlovian blocking and Pavlovian-to-instrumental transfer

Subjects

Thirty-two male (*N* = 22) and female (*N* = 10) Long Evans rats (Charles River) aged approximately 8 weeks at the start of the experiment were used in this study to evaluate the extent to which previously learned cues could block the encoding of novel identity-specific stimulus-outcome memories. Prior to the start of behavioral training, subjects were randomly assigned to Blocking (*N* = 16, 11 male) or Control (*N* = 16, 11 male) groups. Rat were trained and tested using the Outcome-specific blocking and Pavlovian-to-instrumental transfer procedures described above.

Optical stimulation of VTA_{DA}→BLA terminals during Pavlovian blocking

Subjects

Twenty-four male (*N* = 12) and female (*N* = 12) transgenic TH-cre+ (hemizygous) Long Evans rats aged between 9-12 weeks at the time of surgery were used in this study. Subjects with misplaced optical fibers (*N* = 2) or lacking viral expression (*N* = 2) were excluded from the dataset.

Surgery

Th-cre rats were randomly assigned to a viral group and infused bilaterally with a cre-dependent AAV encoding either the excitatory opsin channelrhodopsin (ChR2; *N* = 11, 6 male; AAV5-EF1a-DIO-hChR2(H134R)-eYFP, University of North Carolina Vector Core) or an enhanced yellow fluorescent protein control (eYFP; *N* = 13, 6 males; pAAV5-Ef1a-DIO-eYFP, Addgene). Virus (0.2 µl) was infused bilaterally at a rate of 0.1 µl/min into the VTA (AP: -5.3; ML: ±0.7; DV: -8.3 mm from bregma) using a 28-gauge injector. Injectors were left in place for 10 min following viral infusions. Optical fibers (200 µm core, 0.39 NA, Thorlabs) held in ceramic ferrules (Kientec Systems) were implanted bilaterally in the BLA (AP: -2.7; ML: ±5.0; DV: -8.2 mm from bregma). Experiments commenced approximately 2 weeks after surgery to allow sufficient expression in VTA_{DA}→BLA axon terminals at the time of optical manipulation (7-8 weeks after surgery).

Optogenetic stimulation of VTA_{DA}→BLA projections

Rats received magazine conditioning, instrumental training, and visual cue Pavlovian conditioning as described for the Outcome-specific blocking and Pavlovian-to-instrumental transfer procedures above. All subjects received the blocking condition. Animals were habituated to the optical tether (200 µm, 0.22 NA, Doric Lenses) for at least the last 2 days of instrumental conditioning and the last two days of visual cue Pavlovian conditioning, but no light was delivered. Optogenetic excitation was used to stimulate the activity of ChR2-expressing VTA_{DA} axons and terminals in the BLA at the time of each stimulus-outcome pairing during each compound conditioning session. During each compound conditioning session, blue light (473 nm; 10 mW; 25-ms pulse width) was delivered to the BLA via a laser (Dragon Lasers) for 3 s at a rate of 20 Hz concurrent with each outcome delivery. We selected this stimulation frequency to match the upper end firing rate of VTA_{DA} neurons detected in response to reward[6, 53] similar to prior work on the VTA→BLA pathway[88]. Following compound conditioning, rats proceeded to the PIT test as described above, during which they were tethered to the optical patch cords, but no light was delivered.

Intracranial self-stimulation

Following the PIT test, rats received 2 days of intracranial self-stimulation (ICSS) testing. This occurred in a distinct context from the prior conditioning and testing. This context had a smooth plexiglass rather than grid floor, round right-side wall and no levers or food-delivery port. Each day consisted of one 1-hr session where animals were allowed to nose poke in 2 ports positioned on the left and right side of the left wall of the operant chamber. Nose pokes into the active port triggered 1-s blue light (473nm; 10 mW; 25-ms pulse width; 20 Hz) delivery to the BLA. Subsequent nose pokes during this 1-s light-delivery

period were recorded but did not extend light delivery. Inactive port pokes were also recorded. For half of the subjects in each group, the left port was active and the right inactive, with the opposite arrangement for the other half.

Histology

Following behavioral experiments, rats were deeply anesthetized with Nembutal and transcardially perfused with phosphate buffered saline (PBS) followed by 4% paraformaldehyde (PFA). Brains were removed and post-fixed in 4% PFA overnight, placed into 30% sucrose solution, then sectioned into 30-µm slices using a cryostat and stored in cryoprotectant. Slices were rinsed in a DAPI solution for 4 min (5 mg/mL stock, 1:10000), washed 3 times in PBS for 15 min, mounted on slides and coverslipped with ProLong Gold mounting medium. Images were acquired using a Keyence BZ-X710 microscope (Keyence, El Segundo, CA) with a 4x, 10x, and 20x objective (CFI Plan Apo), CCD camera, and BZ-X Analyze software.

GFP fluorescence was used to confirm expression of GCaMP6f in BLA cell bodies. Immunofluorescence was used to confirm expression of GrabDA2h in the BLA. Floating coronal sections were washed 3 times in 1x PBS for 30 min and then blocked for 1–1.5 hr at room temperature in a solution of 3% normal goat serum and 0.3% Triton X-100 dissolved in PBS. Sections were then washed 3 times in PBS for 15 min and incubated in blocking solution containing chicken anti-GFP polyclonal antibody (1:1000; Abcam, Cambridge, MA) with gentle agitation at 4°C for 18–22 hr. Sections were next rinsed 3 times in PBS for 30 min and incubated with goat anti-chicken IgY, Alexa Fluor 488 conjugate (1:500; Abcam) in blocking solution at room temperature for 2 hr. Sections were washed a final 2 times in PBS for 10 min.

tdTomato fluorescence with a Th costain was used to confirm expression of ArchT-tdTomato in VTA_{DA} neurons. Floating coronal sections were washed 3 times in 1x PBS for 30 min and then blocked for 2 hr at room temperature in a solution of 3% normal donkey serum and 0.2% Triton X-100 dissolved in PBS. Sections were then washed 3 times in PBS for 15 min and incubated in blocking solution containing rabbit anti-TH antibody (1:1000; EMD Millipore, Burlington, MA) with gentle agitation at 4°C for 44-48 hr. Sections were next rinsed 3 times in PBS for 30 min and incubated with goat anti-rabbit IgG, Alexa Fluor 488 conjugate (1:500; Thermofisher Scientific, Waltham, MA) in blocking solution at room temperature for 2 hr. Sections were washed a final 2 times in PBS for 10 min. Immunofluorescence was also used to confirm expression of ArchT-tdTomato in axons and terminals in the BLA. Floating coronal sections were washed 2 times in 1x PBS for 10 min and then blocked for 2 hr at room temperature in a solution of 10% normal goat serum and 0.5% Triton X-100 dissolved in PBS. Sections were then washed 3 times in PBS for 15 min and incubated in blocking solution containing rabbit anti DsRed polyclonal antibody (1:1000; EMD Millipore, Burlington, MA) with gentle agitation at 4°C for 18-22 hr. Sections were next rinsed 3 times in blocking solution for 30 min and incubated with goat anti-rabbit IgG, Alexa Fluor 594 conjugate (1:500; Thermofisher Scientific) in blocking solution at room temperature for 2 hr. Sections were washed a final 2 times in PBS for 10 min.

eYFP fluorescence with a Th costain was used to confirm expression of ChR2-eYFP expression in VTA_{DA} neurons. Staining procedures were as described above using a secondary goat anti-rabbit Alexa 594 antibody (Thermofisher Scientific). Immunofluorescence following procedures described for GFP amplification also described above were used to confirm expression of ChR2 in axons and terminals in the BLA.

Data analysis

Behavioral analysis

Behavioral data were processed with Microsoft Excel (Microsoft, Redmond, WA). Press rates on the last 2 days of instrumental training were averaged across levers then across days and compared between groups to test for any pre-existing group differences in instrumental behavior. Pavlovian conditional food-port approach responses during the Pavlovian and compound conditioning sessions were assessed by comparing the rate of entries into the food-delivery port (entries/min) during the 30-s CS periods relative to the 30-s baseline periods prior to CS onset (preCS). Data were averaged across trials for each CS and then averaged across the CSs. For PIT tests, entry rate into the food-port during the 30-s CSs were

also compared to the baseline 30-s preCS periods. Data were averaged across trials for each CS and then averaged across CSs. Lever press rates (presses/min) during the 30-s baseline preCS periods were compared to that during the 30-s CS periods. Lever presses were separated for presses on the lever that, during training, earned the same outcome as the upcoming or presented cue (Same presses) versus those on the other available lever (Different presses). Data was separated into Same vs Different presses for each preCS and CS period, averaged across trials, then averaged across CS types. To evaluate the cue-induced change in lever pressing, we computed an elevation ratio for each lever [(CS:Same presses)/(CS:Same presses + preCS:Same presses)] and [(CS:Different presses)/(CS:Different presses + preCS:Different presses)]. When two PIT tests were conducted, food-port entry rate, lever-press rates, and elevation ratios were averaged across PIT tests. For ICSS sessions, the total number of nose pokes into the active and active ports were compared across the two sessions.

GCaMP6f fiber photometry analysis

Data were pre-processed using a custom-written pipeline in MATLAB (MathWorks, Natick, MA). Using least-squares linear regression, the 415 nm signal was fit to the 470 nm signal. Change in fluorescence (ΔF/F) at each time point was calculated by subtracting the fitted 415 nm signal from the 470 nm signal and normalizing to the fitted 415 nm data [(470-fitted 415)/fitted 415)]. The ΔF/F data were resampled to 19.5 Hz then Z-scored [(ΔF/F - mean ΔF/F)/std(ΔF/F)]. Using a custom MATLAB workflow, Z-scored traces were then aligned to CS onset for each trial. Peak magnitude was calculated on the Z-scored trace for each trial using 5-s preCS baseline and 5-s postCS onset and postCS offset/outcome delivery windows. Data were averaged across trials and then across CSs. Session data were excluded if no transient calcium fluctuations were detected on the 470 nm channel above the isosbestic channel or if poor linear fit was detected due to excessive motion artifact (N = 2 sessions from N = 2 subjects). To examine the progression in BLA activity across training, we compared data across conditioning sessions 1, 2, 3/4, 5/6, and 7/8. Thus, data from the mid and latter training sessions were averaged across 2-session bins. All subjects had reliable data from at least one session per bin. We were able to obtain reliable imaging data from all the 8 training sessions from N = 6/8 subjects (Figure 1-1).

GrabDA2h fiber photometry analysis

Data were pre-processed using a custom-written pipeline in MATLAB (MathWorks). To account for attenuation in fluorescence resulting from photobleaching across the session, the 470 nm signal was divided by a second-order exponential fitted to the raw data. The data were then resampled to 19.5 Hz and Z-scored. Peak magnitude was calculated on the Z-scored trace for each trial using 5-s preCS baseline and 5-s postCS onset and postCS offset/outcome delivery windows. We compared data across conditioning sessions 1, 2, 3/4, 5/6, and 7/8. Session data were excluded if artifactual signal due to excessive motion or patch cord twisting was detected for at least half of the trials (N = 3 sessions from N = 2 subjects). Two subjects without reliable data from at least one session per bin were excluded. We were able to obtain reliable imaging data from all 8 training sessions from N = 7/9 subjects (Figure 2-1).

Statistical analysis

Datasets were analyzed by two-tailed, paired and unpaired Student's *t* tests, two-, or three-way repeated-measures analysis of variance (ANOVA), as appropriate (GraphPad Prism, GraphPad, San Diego, CA; SPSS, IBM, Chicago, IL). For the few datasets that were slightly non-normal, results were cross-checked using non-parametric statistics and the findings were identical. We opted to use parametric statistics for consistency across experiments and given evidence that ANOVA is robust to slight non-normality[106, 107]. For well-established behavioral effects (PIT), multiple pairwise comparisons were used for *a priori post hoc* comparisons based on a logical extension of Fisher's protected least significant difference procedure for controlling familywise Type I error rates[108]. All other *post hoc* tests were corrected for multiple comparisons using the Bonferroni method and used to clarify main and interaction effects. Greenhouse-Geisser correction was applied to mitigate the influence of unequal variance between conditions. Alpha levels were set at $P < 0.05$.

Sex as a biological variable

Male and female rats were used in approximately equal numbers for each experiment, but the *N* per sex was underpowered to examine sex differences. Sex was therefore not included as a factor in statistical analyses, though individual data points are visually disaggregated by sex.

Rigor and reproducibility

Group sizes were estimated *a priori* based on prior work using male Long Evans rats in this behavioral task[104, 109, 110] and to ensure counterbalancing of CS-outcome and Lever-outcome pairings. Investigators were not blinded to viral group because they were required to administer virus. All behaviors were scored using automated software (MedPC). Each experiment included at least 1 replication cohort and cohorts were balanced by viral group, CS-outcome and Lever-outcome pairings, hemisphere etc. prior to the start of the experiment.

Data and code availability

All data that support the findings of this study are available from the corresponding author upon request. Custom-written MATLAB code is also available from the corresponding author upon request.

SUPPLEMENTAL MATERIALS

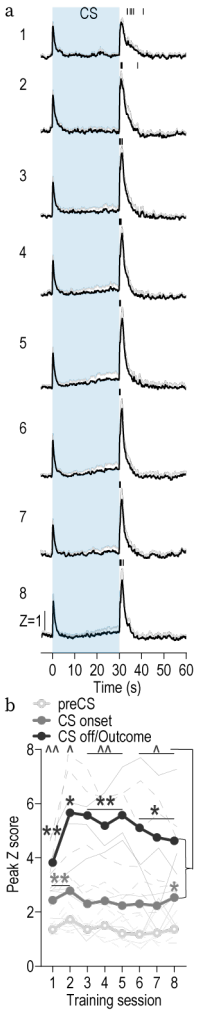

Supplemental Figure 1-1. BLA neurons are active during stimulus-outcome learning across each of the 8 Pavlovian conditioning sessions. (a) Trial-averaged GCaMP6f fluorescence changes (Z-score ΔF/F) in response to CS presentation (blue box) and outcome delivery across each of the 8 Pavlovian conditioning sessions. **(b)** Trial-averaged quantification of maximal (peak) GCaMP Z-score ΔF/F during the 5-s following CS onset or outcome delivery compared to an equivalent baseline period immediately prior CS onset. Thin lines represent individual subjects. BLA neurons respond to both CS onset and offset/outcome delivery, CS offset/outcome responses are larger than those to onset and increase after the first training session (Training x Event: $F_{(3.08, 15.40)} = 3.85$, $P = 0.03$; Event: $F_{(1.18, 5.92)} = 33.57$, $P = 0.001$; Training: $F_{(2.41, 12.06)} = 2.35$, $P = 0.13$). Thin lines represent individual subjects. *$P < 0.05$, **$P < 0.01$ relative to preCS baseline. ^$P < 0.05$, ^^$P < 0.01$ CS offset/outcome relative to CS onset, Bonferroni correction.

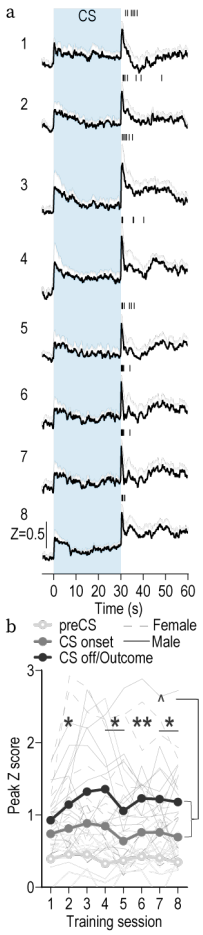

Supplemental Figure 2-1. Dopamine is released in the BLA during stimulus-outcome learning across each of the 8 Pavlovian conditioning sessions. (a) Trial-averaged GrabDA2h fluorescence changes (Z-score) in response to CS presentation (blue box) and outcome delivery across each of the 8 Pavlovian conditioning sessions. **(b)** Trial-averaged quantification of maximal (peak) GrabDA2h fluorescence change Z-score during the 5-s following CS onset or offset/outcome delivery compared to the equivalent baseline period immediately prior CS onset. Thin lines represent individual subjects. Both CS onset and offset/outcome delivery triggered dopamine release in the BLA (Event: $F_{(1.94, 11.65)} = 14.86$, $P = 0.0007$; Training: $F_{(2.91, 17.46)} = 0.47$, $P = 0.70$; Training x Event: $F_{(3.43, 20.60)} = 0.71$, $P = 0.57$). Thin lines represent individual subjects. *$P < 0.05$, **$P < 0.01$ relative to preCS baseline. ^$P < 0.05$ CS offset/outcome relative to CS onset, Bonferroni correction.

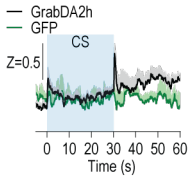

Figure 2-2. GrabDA2h fluorescent changes during stimulus-outcome learning are not due to motion artifact. Trial-averaged GrabDA2h fluorescence changes (Z-scored; *N* = 11) compared to trial-averaged GFP control fluorescence changes (Z-score) from a separate group of subjects (*N* = 3) in response to CS presentation (blue box) and outcome delivery from the 8th Pavlovian conditioning session. Cue onset and outcome responses are only seen for GrabDA2h subjects.

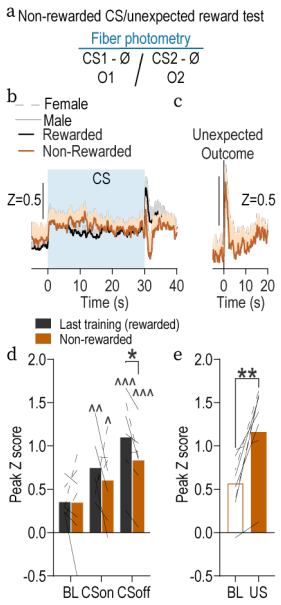

Figure 2-3. Dopamine is released in the BLA in response to predicted and unexpected rewards. **(a)** Procedure schematic. CS, conditioned stimulus (white noise or click); O, outcome (sucrose solution or grain pellet); Ø, no outcome delivery. Following training, in a subset of subjects, cues were delivered without accompanying reward to determine how cue offset altered dopamine release independent of the associated reward. The associated outcome was, instead, delivered unexpectedly 15-s after cue offset. **(b)** Trial-averaged GrabDA fluorescence changes (Z-score) in response to CS presentation (blue box) in the absence of reward compared to the last training session ("Rewarded") in which each CS terminated with reward delivery. Shading reflects between-subjects s.e.m. **(c)** Trial-averaged GrabDA fluorescence changes (Z-score) in response to unexpected reward delivery (averaged across both sucrose and grain pellet trials). **(d)** Trial-averaged quantification of maximal (peak) GrabDA2h fluorescence change Z-score during the 5-s period following CS onset or offset compared to the equivalent baseline period immediately prior to CS onset for both the non-rewarded test and the rewarded last training session. Planned comparisons. *Rewarded v. unrewarded: baseline, $t_{(12)} = 0.06$, $P = 0.95$; CS onset, $t_{(12)} = 1.28$, $P = 0.22$; CS offset, $t_{(12)} = 2.36$, $P = 0.04$. ^Relative to baseline: Rewarded CS onset $t_{(12)} = 3.50$, $P = 0.004$; Rewarded CS offset $t_{(12)} = 6.64$, $P < 0.0001$; Non-rewarded CS onset $t_{(12)} = 2.28$, $P = 0.04$; Non-rewarded CS offset $t_{(12)} = 4.34$, $P = 0.001$. **(e)** Trial-averaged quantification of maximal (peak) GrabDA2h fluorescence change Z-score during the 5-s period following unexpected reward delivery compared to the equivalent immediately preceding baseline period. $t_{(6)} = 3.90$, $P = 0.008$. N = 7, 4 male. We detected dopamine responses to cue offset in the absence of outcome delivery, suggesting that, at least after learning, cue offset itself increases dopamine release in the BLA. This response was, however, smaller than that from the last training session in which outcome delivery did follow cue offset, suggesting that outcome delivery also contributes to BLA dopamine release. Indeed, unexpected outcome delivery also triggered dopamine release in the BLA.

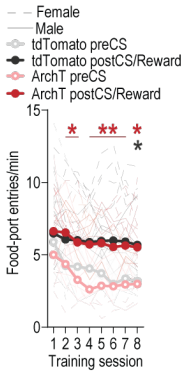

Supplemental Figure 3-1. Inhibition of VTA_{DA}→BLA projections does not disrupt outcome collection during Pavlovian conditioning. There was no effect of optical inhibition of VTA_{DA}→BLA projections at outcome delivery on collection of the food outcomes. Rats entered the food-delivery port during the 30-s postCS/Outcome-delivery period more than the baseline preCS period and similarly between groups (Training: $F_{(3,13),}$ 59.48 = 8.51, $P <$ 0.0001; Period: $F_{(1,19)} = 72.60$, $P <$ 0.0001; Virus: $F_{(1,19)} = 0.47$, $P = 0.50$; Training x Virus: $F_{(7,133)} = 0.65$, $P = 0.72$; Training x Period: $F_{(4.94,93.85)} = 3.00$, $P = 0.02$; Virus x Period: $F_{(1,19)} = 0.87$, $P = 0.36$; Training x Virus x Period: $F_{(7,133)} = 0.71$, $P = 0.66$). *$P < 0.05$, **$P < 0.01$ relative to preCS baseline, Bonferroni correction.

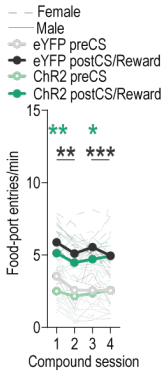

Supplemental Figure 5-1. Stimulation of VTA_{DA}→BLA projections does not affect outcome collection during compound conditioning. There was no effect of optical stimulation of VTA_{DA}→BLA projections paired with outcome delivery on collection of the food outcomes. Rats entered the food-delivery port during the 30-s post-CS/Outcome-delivery period more than the preCS baseline period and similarly between groups (Training: $F_{(1.50,32.90)} = 3.70$, $P = 0.047$; Period: $F_{(1,22)} = 46.80$, $P < 0.0001$; Virus: $F_{(1,22)} = 1.89$, $P = 0.18$; Training x Virus: $F_{(3,66)} = 1.48$, $P = 0.23$; Training x Period: $F_{(2.55,56.04)} = 0.22$, $P = 0.85$; Virus x Period: $F_{(1,22)} = 0.04$, $P = 0.84$; Training x Virus x Period: $F_{(3,66)} = 0.51$, $P = 0.68$). *$P < 0.05$, **$P < 0.01$ relative to preCS baseline, Bonferroni correction.

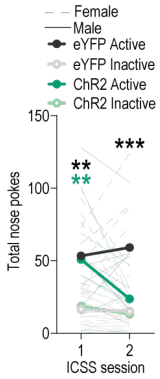

Supplemental Figure 5-2. Stimulation of VTA_{DA}→BLA projections is not reinforcing. To assess the reinforcing properties of VTA_{DA}→BLA activation, rats were given 2 sessions of intracranial self-stimulation (ICSS) in a context different from prior conditioning. Nose pokes in the active port triggered 1-s of blue light delivery (473 nm; 10 mW; 25 ms pulse width; 20 Hz). Data show total active nose pokes compared to inactive nose pokes across 2, 1-hr ICSS sessions. Activation of VTA_{DA}→BLA projections was not reinforcing. Rats expressing ChR2 showed similar levels of active nose pokes as the eYFP control group in the first session and this decreased to the level of the inactive nose pokes in the second session (Session x Virus x Nose poke: $F_{(1, 22)} = 5.00$, $P = 0.04$; Virus x Nose poke: $F_{(1, 22)} = 5.18$, $P = 0.03$; Session x Virus: $F_{(1,22)} = 5.18$, $P = 0.03$; Session x Nose poke: $F_{(1, 22)} = 1.24$, $P = 0.28$; Session: $F_{(1, 22)} = 3.05$, $P = 0.09$; Virus: $F_{(1, 22)} = 1.94$, $P = 0.18$; Nose poke: $F_{(1, 22)} = 54.66$, $P < 0.0001$). $^{*}P < 0.05$, $^{**}P < 0.01$ relative to inactive nose pokes, Bonferroni correction. Elevated active v. inactive port nose poking in both the eYFP and ChR2 groups likely resulted from the prior association formed between blue light and outcome delivery during compound conditioning. This extinguished by the second session in the ChR2 group.